Bull Math Biol (2011) 73: 515–548
DOI 10.1007/s11538-010-9538-z

ORIGINAL ARTICLE

Modelling the Transmission Dynamics and Control of the Novel 2009 Swine Influenza (H1N1) Pandemic

O. Sharomi · C.N. Podder · A.B. Gumel · S.M. Mahmud · E. Rubinstein

Received: 13 November 2009 / Accepted: 15 March 2010 / Published online: 9 April 2010

Abstract The paper presents a deterministic compartmental model for the transmission dynamics of swine influenza (H1N1) pandemic in a population in the presence of an imperfect vaccine and use of drug therapy for confirmed cases. Rigorous analysis of the model, which stratifies the infected population in terms of their risk of developing severe illness, reveals that it exhibits a vaccine-induced backward bifurcation when the associated *reproduction number* is less than unity. The epidemiological consequence of this result is that the effective control of H1N1, when the reproduction number is less than unity, in the population would then be dependent on the initial sizes of the subpopulations of the model. For the case where the vaccine is perfect, it is shown that having the reproduction number less than unity is necessary and sufficient for effective control of H1N1 in the population (in such a case, the associated disease-free equilibrium is globally asymptotically stable). The model has a unique endemic equilibrium when the reproduction number exceeds unity. Numerical simulations of the model, using data relevant to the province of Manitoba, Canada, show that it reasonably mimics the observed H1N1 pandemic data for Manitoba during the first (Spring) wave of the pandemic. Further, it is shown that the timely implementation of a mass vaccination program together with the size of the Manitoban population that have preexisting infection-acquired immunity (from the first wave) are crucial to the magnitude of the expected burden of disease associated with the second wave of

O. Sharomi · C.N. Podder · A.B. Gumel (✉)
Department of Mathematics, University of Manitoba, Winnipeg, Manitoba R3T 2N2, Canada
e-mail: gumelab@cc.umanitoba.ca

S.M. Mahmud
Department of Community Health Sciences, University of Manitoba, Winnipeg, Manitoba R3T 2N2, Canada

E. Rubinstein
Department of Medical Microbiology and Department of Internal Medicine, University of Manitoba, Winnipeg, Manitoba R3T 2N2, Canada

the H1N1 pandemic. With an estimated vaccine efficacy of approximately 80%, it is projected that at least 60% of Manitobans need to be vaccinated in order for the effective control or elimination of the H1N1 pandemic in the province to be feasible. Finally, it is shown that the burden of the second wave of H1N1 is expected to be at least three times that of the first wave, and that the second wave would last until the end of January or early February, 2010.

Keywords Swine flu H1N1 · Model

1 Introduction

The emergence of the H1N1 Influenza A (also known as the swine influenza) pandemic in the Spring of 2009 (Centers for Disease Control and Prevention 2009d; El Universal 2009; GenBank Sequences From 2009 H1N1 Influenza Outbreak 2009; World Health Organization 2009a, 2009b, 2009c) poses major public health challenges globally (World Health Organization 2009b, 2009c). Since its emergence in Mexico in April 2009, the novel H1N1 pandemic, which is believed to have resulted from a recent genetic reassortment involving several influenza virus lineages (Pourbohloul et al. 2009), has so far (as of October 31, 2009) accounted for 441 661 infections and 5712 H1N1-related deaths worldwide (World Health Organization 2009d). The most affected region is the Americas (with 174 565 cases and 4175 deaths). Presently, pandemic influenza transmission remains active in many parts of the tropical zone of the Americas, most notably in several Caribbean countries, and high and increasing rates are reported in the USA and Canada.[1] It is thought that H1N1 spreads in the same way that regular seasonal influenza viruses spread, mainly through coughs and sneezes of people who are infected with the virus, but it may also be spread by touching contaminated objects and then touching the nose or mouth. H1N1 infection has been reported to cause a wide range of flu-like symptoms, including fever, cough, sore throat, body aches, headache, chills and fatigue. In addition, many people also have reported nausea, vomiting and/or diarrhea (Centers for Disease Control and Prevention 2009a).

One disconcerting aspect of the H1N1 pandemic is the higher rates of mortality and severe illness among young healthy individuals, unlike in the case of seasonal influenza which tends to affect older individuals (Chowell et al. 2009; World Health Organization 2009f). In addition, several chronic conditions and behavioral and other risk factors have been associated with increased risk of disease severity among H1N1-infected individuals. Infants and pregnant women (especially in the third trimester) are at increased risk of hospitalization and ICU admissions (Centers for Disease Control and Prevention 2009c; Jamieson et al. 2009; United States Centers for Disease Control and Prevention 2009; World Health Organization 2009g). People with preexisting chronic conditions (such as asthma and

[1] http://healthmap.org/swineflu/. Accessed 02 November 2009.

other chronic lung diseases, chronic kidney and heart diseases, obesity and conditions associated with immune suppression) were found in several analyses to have increased the risk of death and ICU admission (Kumar et al. 2009; United States Centers for Disease Control 2009). In Manitoba, Aboriginals, especially those residing in remote and isolated communities, were at increased risk of severe illness due to pandemic H1N1 infections (Winnipeg Regional Health Authority Report 2009).

Because of the large numbers of those at risk of severe illness and the lack of preexisting immunity to the pandemic virus in the population at large, concerns have been raised about the ability of the health care system to cope with large numbers of patients requiring treatment in intensive care units (ICUs) during the peak period of the "second wave". The second wave of H1N1 is currently underway, at least in Canada (believed to have started around early to mid October, 2009) (Canada Enters Second Wave of H1N1 2009). Several public health measures, including social exclusion (e.g., school closures, banning large gathering etc.), could be possibly deployed to contain the pandemic. Other likely effective measures include mass vaccination and use of antiviral drugs to treat symptomatic individuals during the early phases of illness (Centers for Disease Control and Prevention 2009b). Mass vaccination against H1N1 is on-going in various parts of North America, but current vaccine supply is limited, resulting in prioritization of high-risk groups, which could potentially delay the achievement of effective levels of herd immunity. While there are two effective drugs for the treatment of H1N1, oseltamivir (Tamiflu) and zanamivir (Relenza), their impact on changing the course of the pandemic is unknown, as their availability is also not universal and there are already early reports of oseltamivir-resistant H1N1 strains transmitted (van der Vries et al. 2009). As a result, there is considerable uncertainty about the likely impact of these control measures on the trajectory of the pandemic.

Mathematical models, typically of the form of deterministic or stochastic systems of nonlinear differential equations, have been used to gain insights into the transmission dynamics of emerging and reemerging infectious diseases, such as seasonal and pandemic influenza (see, for instance, Gumel et al. 2008; Miriam et al. 2007), as well as to serve as a public health decision-making tool. Mathematical approaches are useful in studying the qualitative and quantitative dynamics of H1N1 (that is, in estimating its potential burden) and evaluating the impact of public health control strategies, including mass vaccination. A number of modelling studies have already been reported on the transmission dynamics of H1N1 (such as those by Brian et al. 2009; Boëlle et al. 2000; Franco-Paredes and Preciado 2009; Hiroshi et al. 2009; Pourbohloul et al. 2009). Pourbohloul et al. (2009) used a network-based statistical approach to estimate the initial reproduction number of H1N1 influenza in North America. Brian et al. (2009) considered compartmental models to gain insight into the transmission dynamics of H1N1 and the natural history of H1N1 influenza. This study complements the aforementioned studies by designing a new deterministic model, which incorporates an imperfect H1N1 vaccine, drug treatment and stratifies the total infected population in terms of their risk of developing severe illness. The model, which is rigorously analysed to derive important epidemiological thresholds, is used to evaluate the potential burden of the second wave of H1N1 in Manitoba (as of October 17, 2009, Manitoba has reported 927 confirmed cases and 7 H1N1-associated deaths (Manitoba Health 2009)). It is expected that between 10 to 20%

of the total Manitoban population may have preexisting immunity. This estimate is based on preliminary results of a study (led by one of the coauthors: SMM) that estimated the seroprevalence of the pandemic H1N1 infection following the first wave in Manitoba (Mahmud et al. 2010).

The paper is organized as follows. The H1N1 influenza model is formulated in Sect. 2, and rigorously analysed in Sect. 3. Numerical simulations are reported in Sect. 4.

2 Formulation of the Model

The total human population at time t, denoted by $N(t)$, is subdivided into 15 mutually exclusive compartments of susceptible individuals ($S(t)$), vaccinated individuals ($V(t)$), latently infected individuals ($L(t)$), infectious individuals without disease symptoms ($A(t)$), high-risk symptomatic individuals in the early stage (first two days) of infection ($I_1(t)$), low-risk symptomatic individuals in the early stage (first two days) of infection ($Y_1(t)$), high-risk symptomatic individuals in the later stage of infection ($I_2(t)$), low-risk symptomatic individuals in the later stage of infection ($Y_2(t)$), high-risk treated infected individuals ($T_{\mathrm{H}}(t)$), low-risk treated infected individuals ($T_{\mathrm{L}}(t)$), high-risk hospitalized individuals not in the ICU ($H_{\mathrm{H}}(t)$), low-risk hospitalized individuals not in the ICU ($H_{\mathrm{L}}(t)$), high-risk hospitalized individuals in the ICU ($C_{\mathrm{H}}(t)$), low-risk hospitalized individuals in the ICU ($C_{\mathrm{L}}(t)$) and recovered individuals ($R(t)$). Thus,

$$\begin{aligned} N(t) = {} & S(t) + V(t) + L(t) + A(t) + I_1(t) + Y_1(t) + I_2(t) + Y_2(t) \\ & + T_{\mathrm{H}}(t) + T_{\mathrm{L}}(t) + H_{\mathrm{H}}(t) + H_{\mathrm{L}}(t) + C_{\mathrm{H}}(t) + C_{\mathrm{L}}(t) + R(t). \end{aligned}$$

It is worth emphasizing that the model to be designed stratifies the total infected population according to their risk of developing severe illness (i.e., high-risk individuals are more likely to develop severe disease, require hospitalization, ICU admission and suffer increased mortality in comparison to low-risk individuals). The susceptible population is increased by the recruitment of new individuals (assumed susceptible) into the population at a rate Π. Susceptible individuals acquire H1N1 infection (and become latent), following effective contact with infected individuals (i.e., those in the L, A, I_1, I_2, T, H_1 and H_2 classes), at a rate λ, given by

$$\lambda(t) = \frac{\beta[D_1(t) + D_2(t)]}{N(t)}, \tag{1}$$

where

$$\begin{aligned} D_1(t) &= \theta_1 L(t) + I_1(t) + \theta_2 Y_1(t) + \theta_3 I_2(t) + \theta_4 Y_2(t) + \theta_5 A(t) + \theta_6 T_{\mathrm{H}}(t), \\ D_2(t) &= \theta_7 T_{\mathrm{L}}(t) + \theta_8 H_{\mathrm{H}}(t) + \theta_9 H_{\mathrm{L}}(t) + \theta_{10} C_{\mathrm{H}}(t) + \theta_{11} C_{\mathrm{L}}(t). \end{aligned}$$

In (1), β is the effective contact rate. Further, the modification parameters $0 < \theta_i|_{i=1\ldots11} < 1$ account for the assumed decrease in the relative infectiousness of individuals in the L, Y_1, I_2, Y_2, A, T_{H}, T_{L}, H_{H}, H_{L}, C_{H} and C_{L} classes in comparison to

infectious individuals in the early stage of infection (I_1) (it should be mentioned that the model to be designed is robust enough to allow for this assumption to be relaxed for some of the state variables, particularly Y_1, Y_2, I_2 and A). That is, it is assumed that infected individuals in the L, Y_1, I_2, Y_2, A, T_{H}, T_{L}, H_{H}, H_{L}, C_{H} and C_{L} classes are less infectious than infectious individuals in the I_1 class. It is worth stating that it is assumed that latently infected individuals (in the L class) can transmit infection (albeit at a very small rate, $\theta_1\beta$, with $0 < \theta_1 \ll 1$). Furthermore, it is assumed that hospitalized individuals not in ICU (i.e., those in the H_{H} and H_{L} classes) and in ICU (i.e., those in the C_{H} and C_{L} classes) can transmit infection at reduced rates $\theta_8\beta$, $\theta_9\beta$ and $\theta_{10}\beta$, $\theta_{11}\beta$, respectively. These assumptions can be relaxed (if hospital isolation is perfect) by setting $\theta_{10} = \theta_{11} = 0$.

Susceptible individuals are vaccinated at a rate ξ. It is assumed that the vaccine is imperfect, so that vaccinated individuals can acquire breakthrough infection at a reduced rate $(1-\epsilon)\lambda$, where $0 < \epsilon < 1$ is the vaccine efficacy against infection. Latently infected individuals become infectious (typically after 7 days of infection) at a rate α (so that, $1/\alpha = 7$ days). A fraction, r, of these individuals show clinical symptoms of H1N1 (and move to the class I_1), while the remaining fraction, $(1-r)$, will not (but still remain capable of infecting others). The latter group is moved to the class A (of infectious individuals with no disease symptoms). A fraction, f, of individuals who show clinical symptoms of H1N1 are assumed to be of high risk and are moved to the I_1 class, while the remaining fraction, $1-f$, are considered of low risk and moved to the Y_1 class.

Individuals in the I_1 and Y_1 classes move to the later stage of infection (after about 48 hours) at rates κ_{H} and κ_{L}, respectively. Infectious individuals in the classes I_1 and Y_1 are treated, within the 48-hour window, at rates τ_{H} and τ_{L}, respectively. It is assumed that treatment is not effective for infected individuals in the I_2 and Y_2 classes. This study assumes that Tamiflu is only offered therapeutically; and such treatment is only effective if administered within the first 48 hours of infectiousness. Furthermore, since resistance to these drugs has been rare (during this pandemic), the model does not account for the development and transmission of resistant strains (FluWatch 2010).

Individuals in the late stages of H1N1 infection (i.e., those in the I_2 and Y_2 classes) become sick and are hospitalized at rates ψ_{H} and ψ_{L}, respectively. Furthermore, these individuals can recover naturally at rates γ_{H} and γ_{L}, respectively. Infectious individuals that show no symptoms of H1N1 recover naturally at a rate γ_{A}. Treated individuals can fail treatment and become hospitalized at rates ϕ_{H} and ϕ_{L}, respectively; otherwise, they recover at rates γ_{TH} and γ_{TL} respectively. Hospitalized individuals, both of high and low risk, recover at rates γ_{HH} and γ_{HL}, respectively, or are transferred to the ICU (of high or low risk) at rates σ_{H} and σ_{L}, respectively. ICU patients (both in high- and low-risk classes) can recover at rates γ_{CH} and γ_{CL}, respectively. Natural mortality occurs in all classes at a rate μ, while hospitalized individuals (in the H_{H} and H_{L} classes) and those in ICU (i.e., those in the C_{H} and C_{L} classes) suffer additional disease-induced death at rates δ_{HH}, δ_{HL}, δ_{CH} andδ_{CL}, respectively. It is assumed that $\delta_{\mathrm{CH}} > \delta_{\mathrm{HH}}$ and $\delta_{\mathrm{CL}} > \delta_{\mathrm{HL}}$, since individuals in ICU (either of high or low risk) are more likely to die than those not in ICU (because of their severe complications). Furthermore, it is assumed that recovered individuals do not lose their infection-acquired immunity, so that they do not become susceptible to reinfection.

Combining all the aforementioned definitions and assumptions, it follows that the model for the transmission dynamics of H1N1 flu in a population is given by the following deterministic system of nonlinear differential equations (see Fig. 1 for a flow diagram and Table 1 for the description of the variables and parameters of the model):

$$
\begin{aligned}
\frac{dS}{dt} &= \Pi - \lambda(t)S(t) - k_1 S(t),\\
\frac{dV}{dt} &= \xi S(t) - (1-\epsilon)\lambda(t)V(t) - \mu V(t),\\
\frac{dL}{dt} &= \lambda(t)S(t) + (1-\epsilon)\lambda(t)V(t) - k_2 L(t),\\
\frac{dI_1}{dt} &= fr\alpha L(t) - k_3 I_1(t),\\
\frac{dY_1}{dt} &= (1-f)r\alpha L(t) - k_4 Y_1(t),\\
\frac{dI_2}{dt} &= \kappa_{\mathrm{H}} I_1(t) - k_5 I_2(t),\\
\frac{dY_2}{dt} &= \kappa_{\mathrm{L}} Y_1(t) - k_6 Y_2(t),\\
\frac{dA}{dt} &= (1-r)\alpha L(t) - k_7 A(t),\\
\frac{dT_{\mathrm{H}}}{dt} &= \tau_{\mathrm{H}} I_1(t) - k_8 T_{\mathrm{H}}(t),\\
\frac{dT_{\mathrm{L}}}{dt} &= \tau_{\mathrm{L}} Y_1(t) - k_9 T_{\mathrm{L}}(t),\\
\frac{dH_{\mathrm{H}}}{dt} &= \psi_{\mathrm{H}} I_2(t) + \phi_{\mathrm{H}} T_{\mathrm{H}}(t) - k_{10} H_{\mathrm{H}}(t),\\
\frac{dH_{\mathrm{L}}}{dt} &= \psi_{\mathrm{L}} Y_2(t) + \phi_{\mathrm{L}} T_{\mathrm{L}}(t) - k_{11} H_{\mathrm{L}}(t),\\
\frac{dC_{\mathrm{H}}}{dt} &= \sigma_{\mathrm{H}} H_{\mathrm{H}}(t) - k_{12} C_{\mathrm{H}}(t),\\
\frac{dC_{\mathrm{L}}}{dt} &= \sigma_{\mathrm{L}} H_{\mathrm{L}}(t) - k_{13} C_{\mathrm{L}}(t),\\
\frac{dR}{dt} &= \gamma_{\mathrm{H}} I_2(t) + \gamma_{\mathrm{L}} Y_2(t) + \gamma_{\mathrm{A}} A(t) + \gamma_{\mathrm{TH}} T_{\mathrm{H}}(t) + \gamma_{\mathrm{TL}} T_{\mathrm{L}}(t)\\
&\quad + \gamma_{\mathrm{HH}} H_{\mathrm{H}}(t) + \gamma_{\mathrm{HL}} H_{\mathrm{L}}(t) + \gamma_{\mathrm{CH}} C_{\mathrm{H}}(t) + \gamma_{\mathrm{CL}} C_{\mathrm{L}}(t) - \mu R(t),
\end{aligned}
\tag{2}
$$

where

$$
k_1 = \mu + \xi, \qquad k_2 = \mu + \alpha, \qquad k_3 = \mu + \tau_{\mathrm{H}} + \kappa_{\mathrm{H}}, \qquad k_4 = \mu + \tau_{\mathrm{L}} + \kappa_{\mathrm{L}},
$$

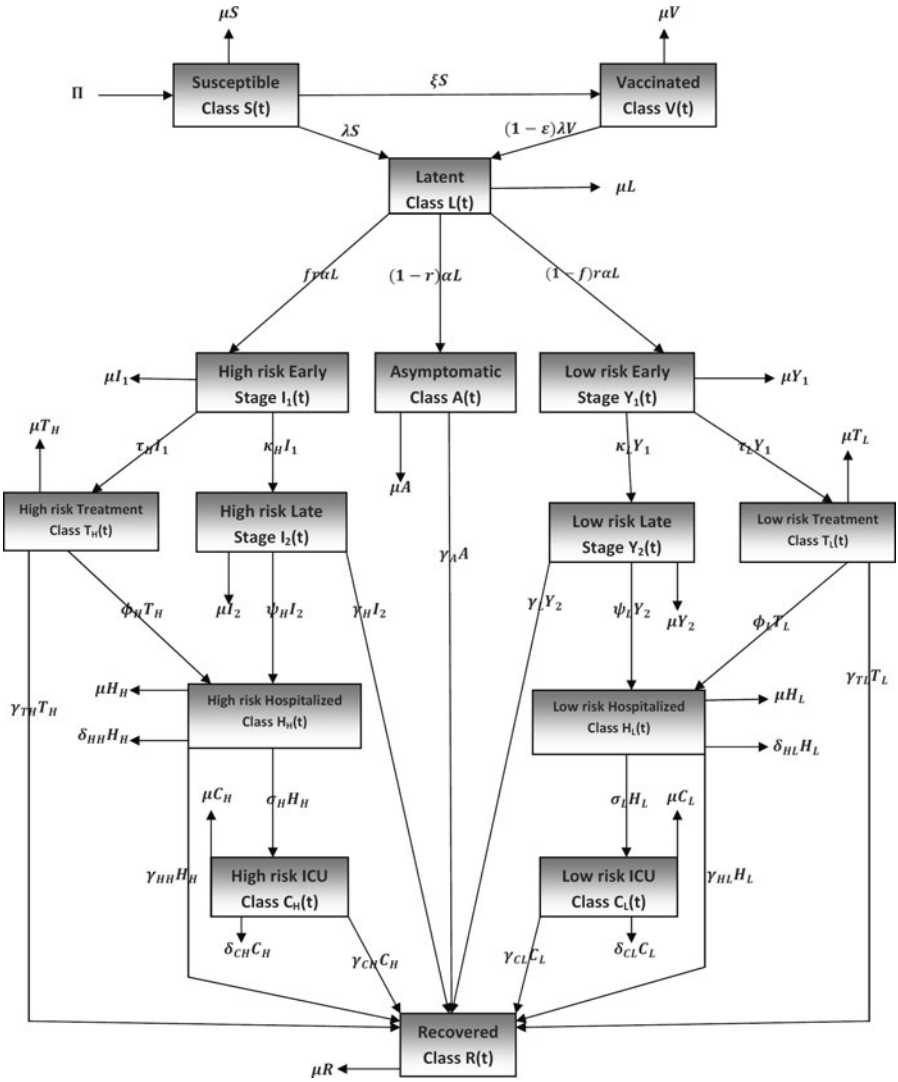

Fig. 1 Flow diagram of the model

$$k_5 = \mu + \psi_{\mathrm{H}} + \gamma_{\mathrm{H}}, \qquad k_6 = \mu + \psi_{\mathrm{L}} + \gamma_{\mathrm{L}}, \qquad k_7 = \mu + \gamma_{\mathrm{A}},$$
$$k_8 = \mu + \phi_{\mathrm{H}} + \gamma_{\mathrm{TH}}, \qquad k_9 = \mu + \phi_{\mathrm{L}} + \gamma_{\mathrm{TL}},$$
$$k_{10} = \mu + \sigma_{\mathrm{H}} + \gamma_{\mathrm{HH}} + \delta_{\mathrm{HH}}, \qquad k_{11} = \mu + \sigma_{\mathrm{L}} + \gamma_{\mathrm{HL}} + \delta_{\mathrm{HL}},$$
$$k_{12} = \mu + \gamma_{\mathrm{CH}} + \delta_{\mathrm{CH}}, \qquad k_{13} = \mu + \gamma_{\mathrm{CL}} + \delta_{\mathrm{CL}}.$$

It is worth mentioning that one limitation of model (2) is that it does not explicitly incorporate the role of age structure (to account for the variability in susceptibility according to age). A homogeneously mixed population is assumed to allow for the

Table 1 Description of variables and parameters of the model

Variable	Description
$S(t)$	Susceptible individuals
$V(t)$	Vaccinated individuals
$L(t)$	Latently infected individuals
$I_1(t)$	High-risk symptomatic individuals in early stage of infectiousness
$Y_1(t)$	Low-risk symptomatic individuals in early stage of infectiousness
$I_2(t)$	High-risk symptomatic individuals in late stage of infectiousness
$Y_2(t)$	Low-risk symptomatic individuals in late stage of infectiousness
$A(t)$	Infectious individuals with no symptoms
$T_{\mathrm{H}}(t)$	High-risk treated infected individuals
$T_{\mathrm{L}}(t)$	Low-risk treated infected individuals
$H_{\mathrm{H}}(t)$	High-risk hospitalized individuals not in ICU
$H_{\mathrm{L}}(t)$	Low-risk hospitalized individuals not in ICU
$C_{\mathrm{H}}(t)$	High-risk hospitalized individuals in ICU
$C_{\mathrm{L}}(t)$	Low-risk hospitalized individuals in ICU
$R(t)$	Recovered individuals
Parameter	**Description (per day)**
Π	Recruitment rate into the susceptible population
μ	Natural death rate
β	Effective contact rate
$\delta_{\mathrm{HH}}, \delta_{\mathrm{HL}}, \delta_{\mathrm{CH}}, \delta_{\mathrm{CL}}$	Disease-induced mortality for individuals in $H_{\mathrm{H}}, H_{\mathrm{L}}$ and $C_{\mathrm{H}}, C_{\mathrm{L}}$ classes, respectively
ξ	Vaccination rate
ϵ	Vaccine efficacy
α	Rate at which latent individuals become infectious
r	Fraction of infectious individuals who show disease symptoms
f	Fraction of infectious individuals showing symptoms with high risk
κ_{H}	Progression rate of infectious individuals from I_1 to I_2
κ_{L}	Progression rate of infectious individuals from Y_1 to Y_2
$\gamma_{\mathrm{H}}, \gamma_{\mathrm{L}}, \gamma_{\mathrm{A}}, \gamma_{\mathrm{TH}}, \gamma_{\mathrm{TL}}$	Recovery rates for individuals in $I_2, Y_2, A, T_{\mathrm{H}}, T_{\mathrm{L}}$ classes, respectively
$\gamma_{\mathrm{HH}}, \gamma_{\mathrm{HL}}, \gamma_{\mathrm{CH}}, \gamma_{\mathrm{CL}}$	Recovery rates for individuals in $H_{\mathrm{H}}, H_{\mathrm{L}}, C_{\mathrm{H}}$ and C_{L} classes, respectively
$\psi_{\mathrm{H}}, \psi_{\mathrm{L}}$	Hospitalization rate for individuals in I_2 and Y_2 classes, respectively
$\phi_{\mathrm{H}}, \phi_{\mathrm{L}}$	Hospitalization rate for high- and low-risk treated individuals, respectively.
$\sigma_{\mathrm{H}}, \sigma_{\mathrm{L}}$	ICU admission rate for high- and low-risk hospitalized individuals, respectively
$\tau_{\mathrm{H}}, \tau_{\mathrm{L}}$	Treatment rate for individuals in I_1 and Y_1 classes, respectively
θ_i $(i = 1 \ldots 11)$	Relative risk of infectiousness of infected individuals in relation to those in I_1 class

ensuing mathematical analysis of the model to be more tractable. We intend to investigate the issue of heterogeneity, in the context of the H1N1 pandemic, in a future study.

3 Analysis of the Model

3.1 Basic Properties

3.1.1 Positivity and Boundedness of Solutions

For the basic model (2) to be epidemiologically meaningful, it is important to prove that all its state variables are nonnegative for all time. In other words, solutions of the model system (2) with positive initial data will remain positive for all time $t > 0$.

Theorem 1 *Let the initial data* $S(0) > 0$, $V(0) \geq 0$, $L(0) \geq 0$, $I_1(0) \geq 0$, $Y_1(0) \geq 0$, $I_2(0) \geq 0$, $Y_2(0) \geq 0$, $A(0) \geq 0$, $T_{\mathrm{H}}(0) \geq 0$, $T_{\mathrm{L}}(0) \geq 0$, $H_{\mathrm{H}}(0) \geq 0$, $H_{\mathrm{L}}(0) \geq 0$, $C_{\mathrm{H}}(0) \geq 0$, $C_{\mathrm{L}}(0) \geq 0$, $R(0) \geq 0$. *Then the solutions* $(S, V, L, I_1, Y_1, I_2, Y_2, A, T_{\mathrm{H}}, T_{\mathrm{L}}, H_{\mathrm{H}}, H_{\mathrm{L}}, C_{\mathrm{H}}, C_{\mathrm{L}}, R)$ *of the basic model* (2) *are positive for all* $t > 0$. *Furthermore*,

$$\limsup_{t\to\infty} N(t) \leq \frac{\Pi}{\mu},$$
$$\text{with } N = S + V + L + I_1 + Y_1 + I_2 + Y_2 + A + T_{\mathrm{H}} + T_{\mathrm{L}} + H_{\mathrm{H}} + H_{\mathrm{L}} + C_{\mathrm{H}} + C_{\mathrm{L}} + R.$$

Proof It follows, from the first equation of system (2), that

$$\frac{d}{dt}\left[S(t)\exp\left\{\int_0^t \lambda(u)\,du + (\mu+\xi)t\right\}\right] = \Pi\exp\left\{\int_0^t \lambda(u)\,du + (\mu+\xi)t\right\}.$$

Hence,

$$\begin{aligned} &S(t_1)\exp\left\{\int_0^{t_1} \lambda(u)\,du + (\mu+\xi)t_1\right\} - S(0) \\ &\quad = \int_0^{t_1} \Pi\exp\left\{\int_0^x \lambda(v)\,dv + (\mu+\xi)x\right\}dx, \end{aligned}$$

so that

$$\begin{aligned} S(t_1) &= S(0)\exp\left\{-\int_0^{t_1} \lambda(u)\,du + (\mu+\xi)t_1\right\} \\ &\quad + \exp\left\{-\int_0^{t_1} \lambda(u)\,du + (\mu+\xi)t_1\right\} \\ &\quad \times \int_0^{t_1} \Pi\exp\left\{\int_0^x \lambda(v)\,dv + (\mu+\xi)x\right\}dx. \\ &> 0. \end{aligned}$$

Similarly, it can be shown that $V \geq 0$, $L \geq 0$, $I_1 \geq 0$, $Y_1 \geq 0$, $I_2 \geq 0$, $Y_2 \geq 0$, $A \geq 0$, $T_{\mathrm{H}} \geq 0$, $T_{\mathrm{L}} \geq 0$, $H_{\mathrm{H}} \geq 0$, $H_{\mathrm{L}} \geq 0$, $C_{\mathrm{H}} \geq 0$, $C_{\mathrm{L}} \geq 0$ and $R \geq 0$ for all $t > 0$. For

the second part of the proof, it should be noted, first of all, that $0 < H_{\mathrm{H}}(t) \leq N(t)$, $0 < H_{\mathrm{L}}(t) \leq N(t)$, $0 < C_{\mathrm{H}}(t) \leq N(t)$ and $0 < C_{\mathrm{L}}(t) \leq N(t)$.

Adding all the equations in the differential equation system (2) gives

$$\frac{dN}{dt} = \Pi - \mu N(t) - \delta_{\mathrm{HH}} H_{\mathrm{H}}(t) - \delta_{\mathrm{HL}} H_{\mathrm{L}}(t) - \delta_{\mathrm{CH}} C_{\mathrm{H}}(t) - \delta_{\mathrm{CL}} C_{\mathrm{L}}(t). \tag{3}$$

It follows from (3) that

$$\Pi - (\mu + \delta_{\mathrm{HH}} + \delta_{\mathrm{HL}} + \delta_{\mathrm{CH}} + \delta_{\mathrm{CL}}) N(t) \leq \frac{dN}{dt} < \Pi - \mu N(t).$$

Thus,

$$\frac{\Pi}{\mu + \delta_{\mathrm{HH}} + \delta_{\mathrm{HL}} + \delta_{\mathrm{CH}} + \delta_{\mathrm{CL}}} \leq \liminf_{t \to \infty} N(t) \leq \limsup_{t \to \infty} N(t) \leq \frac{\Pi}{\mu},$$

so that

$$\limsup_{t \to \infty} N(t) \leq \frac{\Pi}{\mu},$$

as required. □

3.1.2 Invariant Regions

Model (2) will be analysed in a biologically-feasible region as follows. We first show that system (2) is dissipative (i.e., all feasible solutions are uniformly bounded in a proper subset $\mathcal{D} \subset \mathbb{R}_+^{15}$). Consider the region

$$\mathcal{D} = \Big\{ (S, V, L, I_1, Y_1, I_2, Y_2, A, T_{\mathrm{H}}, T_{\mathrm{L}}, H_{\mathrm{H}}, H_{\mathrm{L}}, C_{\mathrm{H}}, C_{\mathrm{L}}, R) \in \mathbb{R}_+^{15} : \\ S + V + L + I_1 + Y_1 + I_2 + Y_2 + A + T_{\mathrm{H}} + T_{\mathrm{L}} + H_{\mathrm{H}} + H_{\mathrm{L}} + C_{\mathrm{H}} \\ + C_{\mathrm{L}} + R \leq \frac{\Pi}{\mu} \Big\}.$$

The following steps are followed to establish the positive invariance of $\mathcal{D}$ (i.e., solutions in $\mathcal{D}$ remain in $\mathcal{D}$ for all $t \geq 0$). It follows from (3) that

$$\frac{dN}{dt} \leq \Pi - \mu N(t). \tag{4}$$

A standard comparison theorem (Lakshmikantham et al. 1989) can then be used to show that $N(t) \leq N(0)e^{-\mu t} + \frac{\Pi}{\mu}(1 - e^{-\mu t})$. In particular, $N(t) \leq \frac{\Pi}{\mu}$ if $N(0) \leq \frac{\Pi}{\mu}$. Thus, the region $\mathcal{D}$ is positively invariant. Hence, it is sufficient to consider the dynamics of the flow generated by (2) in $\mathcal{D}$. In this region, the model can be considered as been epidemiologically and mathematically well posed (Hethcote 2000). Thus, every solution of the basic model (2) with initial conditions in $\mathcal{D}$ remains in $\mathcal{D}$ for all $t > 0$. Therefore, the ω-limit sets of the system (2) are contained in $\mathcal{D}$. This result is summarized below.

Lemma 1 *The region $\mathcal{D}$ is positively invariant for the basic model* (2) *with initial conditions in* $\mathbb{R}_+^{15}$.

3.2 Stability of Disease-Free Equilibrium (DFE)

3.2.1 Local Stability

Model (2) has a DFE, obtained by setting the right-hand sides of the equations in the model to zero, given by

$$\begin{aligned}\mathcal{E}_0 &= \left(S^*, V^*, L^*, I_1^*, Y_1^*, I_2^*, Y_2^*, A^*, T_{\mathrm{H}}^*, T_{\mathrm{L}}^*, H_{\mathrm{H}}^*, H_{\mathrm{L}}^*, C_{\mathrm{H}}^*, C_{\mathrm{L}}^*, R^*\right)\\ &= \left(\frac{\Pi}{k_1}, \frac{\xi\Pi}{\mu k_1}, 0, 0, 0, 0, 0, 0, 0, 0, 0, 0, 0, 0, 0\right). \qquad (5)\end{aligned}$$

The linear stability of $\mathcal{E}_0$ can be established using the next-generation operator method on system (2). Using the notation in (van den Driessche and Watmough 2002), the matrices F and V, for the new infection terms and the remaining transfer terms, are, respectively, given by

$$F = \begin{pmatrix} F_1 & F_2 \\ F_3 & F_4 \end{pmatrix} \quad \text{and} \quad V = \begin{pmatrix} V_1 & V_2 \\ V_3 & V_4 \end{pmatrix},$$

with

$$F_1 = \begin{bmatrix} \beta^*\theta_1 & \beta^* & \beta^*\theta_2 & \beta^*\theta_3 & \beta^*\theta_4 & \beta^*\theta_5 \\ 0 & 0 & 0 & 0 & 0 & 0 \\ 0 & 0 & 0 & 0 & 0 & 0 \\ 0 & 0 & 0 & 0 & 0 & 0 \\ 0 & 0 & 0 & 0 & 0 & 0 \\ 0 & 0 & 0 & 0 & 0 & 0 \end{bmatrix},$$

$$F_2 = \begin{bmatrix} \beta^*\theta_6 & \beta^*\theta_7 & \beta^*\theta_8 & \beta^*\theta_9 & \beta^*\theta_{10} & \beta^*\theta_{11} \\ 0 & 0 & 0 & 0 & 0 & 0 \\ 0 & 0 & 0 & 0 & 0 & 0 \\ 0 & 0 & 0 & 0 & 0 & 0 \\ 0 & 0 & 0 & 0 & 0 & 0 \\ 0 & 0 & 0 & 0 & 0 & 0 \end{bmatrix},$$

$$F_3 = [0]_{6\times 6}, \qquad F_4 = [0]_{6\times 6},$$

$$V_1 = \begin{bmatrix} k_2 & 0 & 0 & 0 & 0 & 0 \\ -fr\alpha & k_3 & 0 & 0 & 0 & 0 \\ -(1-f)r\alpha & 0 & k_4 & 0 & 0 & 0 \\ 0 & -\kappa_{\mathrm{H}} & 0 & K_5 & 0 & 0 \\ 0 & 0 & -\kappa_{\mathrm{L}} & 0 & k_6 & 0 \\ -(1-r)\alpha & 0 & 0 & 0 & 0 & k_7 \end{bmatrix},$$

$$V_2 = [\mathbf{0}]_{6\times 6},$$

$$V_3 = \begin{bmatrix} 0 & -\tau_{\mathrm{H}} & 0 & 0 & 0 & 0 \\ 0 & 0 & -\tau_{\mathrm{L}} & 0 & 0 & 0 \\ 0 & 0 & 0 & -\psi_{\mathrm{H}} & 0 & 0 \\ 0 & 0 & 0 & 0 & -\psi_{\mathrm{L}} & 0 \\ 0 & 0 & 0 & 0 & 0 & 0 \\ 0 & 0 & 0 & 0 & 0 & 0 \end{bmatrix}, \quad \text{and}$$

$$V_4 = \begin{bmatrix} k_8 & 0 & 0 & 0 & 0 & 0 \\ 0 & k_9 & 0 & 0 & 0 & 0 \\ -\phi_{\mathrm{H}} & 0 & k_{10} & 0 & 0 & 0 \\ 0 & -\phi_{\mathrm{L}} & 0 & k_{11} & 0 & 0 \\ 0 & 0 & -\sigma_{\mathrm{H}} & 0 & k_{12} & 0 \\ 0 & 0 & 0 & -\sigma_{\mathrm{L}} & 0 & k_{13} \end{bmatrix},$$

where

$$\beta^* = \frac{\beta[S^* + (1-\epsilon)V^*]}{N^*}.$$

Thus,

$$\mathcal{R}_c = \rho\big(FV^{-1}\big) = \frac{\beta^*(\Phi_1\tau_{\mathrm{H}} + \Phi_2\tau_{\mathrm{L}} + \Phi_3\kappa_{\mathrm{H}} + \Phi_4\kappa_{\mathrm{L}} + \Phi_5)}{k_2k_3k_4k_5k_6k_7k_8k_9k_{10}k_{11}k_{12}k_{13}},$$

where

$$\Phi_1 = fr\alpha k_4k_5k_6k_7k_9k_{11}k_{13}(\theta_6k_{10}k_{12} + \theta_{10}\sigma_{\mathrm{H}}\phi_{\mathrm{H}} + \theta_8k_{12}\phi_{\mathrm{H}}),$$

$$\Phi_2 = r\alpha k_3k_5k_6k_7k_8k_{10}k_{12}(1-f)(\theta_7k_{11}k_{13} + \theta_{11}\sigma_{\mathrm{L}}\phi_{\mathrm{L}} + \theta_9k_{13}\phi_{\mathrm{L}}),$$

$$\Phi_3 = fr\alpha k_4k_6k_7k_8k_9k_{11}k_{13}(\theta_3k_{10}k_{12} + \theta_{10}\sigma_{\mathrm{H}}\psi_{\mathrm{H}} + \theta_8k_{12}\psi_{\mathrm{H}}),$$

$$\Phi_4 = r\alpha k_3k_5k_7k_8k_9k_{10}k_{12}(1-f)(\theta_4k_{11}k_{13} + \theta_{11}\sigma_{\mathrm{L}}\psi_{\mathrm{L}} + \theta_9k_{13}\psi_{\mathrm{L}}),$$

$$\Phi_5 = k_5k_6k_8k_9k_{10}k_{11}k_{12}k_{13}\big[\theta_1k_3k_4k_7 + fr\alpha k_4k_7 + \theta_2(1-f)r\alpha k_3k_7 + \theta_5(1-r)\alpha k_3k_4\big],$$

and ρ represents the spectral radius. Consequently, it follows from Theorem 2 of van den Driessche and Watmough (2002) that:

Lemma 2 *The DFE of the model* (2), *given by* (5), *is locally asymptotically stable* (*LAS*) *whenever* $\mathcal{R}_c < 1$ *and unstable if* $\mathcal{R}_c > 1$.

The threshold quantity, $\mathcal{R}_c$, is the *effective reproduction number* for H1N1 infection. It measures the average number of new H1N1 cases generated by a single infected individual in a population where some of the susceptible individuals are vaccinated (Hethcote 2000; van den Driessche and Watmough 2002).

3.3 Existence of Backward Bifurcation

The phenomenon of backward bifurcation in disease transmission models, where a stable endemic equilibrium coexists with a stable disease-free equilibrium when the associated reproduction number is less than unity, has been observed in numerous disease transmission models such as those for behavioral responses to perceived risks (Hadeler and Castillo-Chavez 1995), multigroup models (Castillo-Chavez et al. 1989a, 1989b; Simon and Jacquez 1992), vaccination models (Brauer 2004; Elbasha and Gumel 2006; Kribs-Zaleta and Valesco-Hernandez 2000; Sharomi et al. 2007), treatment (Sharomi and Gumel 2009; Wang 2006) and models of the transmission of mycobacterium tuberculosis with exogenous reinfection (Castillo-Chavez and Song 2004; Feng et al. 2000) and HTLV-I (Gomez-Acevedo and Li 2005). The epidemiological implication of backward bifurcation is that effective disease control is only feasible if the associated reproduction number is reduced further to values below another subthreshold less than unity. Clearly, this phenomenon has important public health implications, since it renders the classical epidemiological requirement of having the reproduction number less than unity, while necessary, to be insufficient (in general) for disease elimination. Thus, it is instructive to check the possibility of the backward bifurcation phenomenon in the context of the transmission dynamics of the H1N1 pandemic in the presence of an imperfect vaccine.

First of all, the possible equilibrium solutions model (2) can have are determined as follows. Let

$$\mathcal{E}_1 = \left(S^{**}, V^{**}, L^{**}, I_1^{**}, Y_1^{**}, I_2^{**}, Y_2^{**}, A^{**}, T_{\mathrm{H}}^{**}, T_{\mathrm{L}}^{**}, H_{\mathrm{H}}^{**}, H_{\mathrm{L}}^{**}, C_{\mathrm{H}}^{**}, C_{\mathrm{L}}^{**}, R^{**}\right)$$

be any arbitrary equilibrium of model (2). Further, let

$$\lambda^{**} = \frac{\beta(D_1^{**} + D_2^{**})}{N^{**}}, \tag{6}$$

with

$$\begin{aligned} D_1^{**} &= \theta_1 L^{**} + I_1^{**} + \theta_2 Y_1^{**} + \theta_3 I_2^{**} + \theta_4 Y_2^{**} + \theta_5 A^{**} + \theta_6 T_{\mathrm{H}}^{**}, \\ D_2^{**} &= \theta_7 T_{\mathrm{L}}^{**} + \theta_8 H_{\mathrm{H}}^{**} + \theta_9 H_{\mathrm{L}}^{**} + \theta_{10} C_{\mathrm{H}}^{**} + \theta_{11} C_{\mathrm{L}}^{**}, \end{aligned}$$

be the associated force of infection at steady state. To find conditions for the existence of an equilibrium for which H1N1 infection is endemic in the population (i.e., at least one of the subpopulations L^{**}, I_1^{**}, Y_1^{**}, I_2^{**}, Y_2^{**}, A^{**}, T_{H}^{**}, T_{L}^{**}, H_{H}^{**}, H_{L}^{**}, C_{H}^{**} and C_{L}^{**} is nonzero), the equations in (2) are solved in terms of the aforementioned force of infection at steady state (λ^{**}). Setting the right-hand sides of model (2) to zero (at steady state) gives

$$V^{**} = \frac{\xi S^{**}}{\mu + (1-\epsilon)\lambda^{**}}, \qquad L^{**} = \frac{1}{k_2}\left[1 + \frac{\xi(1-\epsilon)}{\mu + (1-\epsilon)\lambda^{**}}\right]\lambda^{**} S^{**},$$

$$I_1^{**} = D_{11}\left[1 + \frac{\xi(1-\epsilon)}{\mu + (1-\epsilon)\lambda^{**}}\right]\lambda^{**} S^{**},$$

$$
\begin{aligned}
Y_1^{**} &= D_{12}\left[1+\frac{\xi(1-\epsilon)}{\mu+(1-\epsilon)\lambda^{**}}\right]\lambda^{**}S^{**},\\
I_2^{**} &= D_{13}\left[1+\frac{\xi(1-\epsilon)}{\mu+(1-\epsilon)\lambda^{**}}\right]\lambda^{**}S^{**},\\
Y_2^{**} &= D_{14}\left[1+\frac{\xi(1-\epsilon)}{\mu+(1-\epsilon)\lambda^{**}}\right]\lambda^{**}S^{**},\\
A^{**} &= D_{15}\left[1+\frac{\xi(1-\epsilon)}{\mu+(1-\epsilon)\lambda^{**}}\right]\lambda^{**}S^{**},\\
T_{\mathrm{H}}^{**} &= D_{16}\left[1+\frac{\xi(1-\epsilon)}{\mu+(1-\epsilon)\lambda^{**}}\right]\lambda^{**}S^{**},\\
T_{\mathrm{L}}^{**} &= D_{17}\left[1+\frac{\xi(1-\epsilon)}{\mu+(1-\epsilon)\lambda^{**}}\right]\lambda^{**}S^{**},\\
H_{\mathrm{H}}^{**} &= D_{18}\left[1+\frac{\xi(1-\epsilon)}{\mu+(1-\epsilon)\lambda^{**}}\right]\lambda^{**}S^{**},\\
H_{\mathrm{L}}^{**} &= D_{19}\left[1+\frac{\xi(1-\epsilon)}{\mu+(1-\epsilon)\lambda^{**}}\right]\lambda^{**}S^{**},\\
C_{\mathrm{H}}^{**} &= D_{20}\left[1+\frac{\xi(1-\epsilon)}{\mu+(1-\epsilon)\lambda^{**}}\right]\lambda^{**}S^{**},\\
C_{\mathrm{L}}^{**} &= D_{21}\left[1+\frac{\xi(1-\epsilon)}{\mu+(1-\epsilon)\lambda^{**}}\right]\lambda^{**}S^{**},\\
R^{**} &= D_{22}\left[1+\frac{\xi(1-\epsilon)}{\mu+(1-\epsilon)\lambda^{**}}\right]\lambda^{**}S^{**},
\end{aligned}
\tag{7}
$$

where

$$
\begin{aligned}
&D_{11}=\frac{fr\alpha}{k_2k_3}, \qquad D_{12}=\frac{(1-f)r\alpha}{k_2k_4}, \qquad D_{13}=\frac{\kappa_{\mathrm{H}}fr\alpha}{k_2k_3k_5},\\
&D_{14}=\frac{\kappa_{\mathrm{L}}(1-f)r\alpha}{k_2k_4k_6}, \qquad D_{15}=\frac{(1-r)\alpha}{k_2k_7}, \qquad D_{16}=\frac{\tau_{\mathrm{H}}fr\alpha}{k_2k_3k_8},\\
&D_{17}=\frac{\tau_{\mathrm{L}}(1-f)r\alpha}{k_2k_4k_9}, \qquad D_{18}=\frac{fr\alpha}{k_2k_3k_{10}}\left(\frac{\psi_{\mathrm{H}}\kappa_{\mathrm{H}}}{k_5}+\frac{\phi_{\mathrm{H}}\tau_{\mathrm{H}}}{k_8}\right),\\
&D_{19}=\frac{(1-f)r\alpha}{k_2k_4k_{11}}\left(\frac{\psi_{\mathrm{L}}\kappa_{\mathrm{L}}}{k_6}+\frac{\phi_{\mathrm{L}}\tau_{\mathrm{L}}}{k_9}\right),\\
&D_{20}=\frac{fr\alpha\sigma_{\mathrm{H}}}{k_2k_3k_{10}k_{12}}\left(\frac{\psi_{\mathrm{H}}\kappa_{\mathrm{H}}}{k_5}+\frac{\phi_{\mathrm{H}}\tau_{\mathrm{H}}}{k_8}\right),\\
&D_{21}=\frac{(1-f)r\alpha\sigma_{\mathrm{L}}}{k_2k_4k_{11}k_{13}}\left(\frac{\psi_{\mathrm{L}}\kappa_{\mathrm{L}}}{k_6}+\frac{\phi_{\mathrm{L}}\tau_{\mathrm{L}}}{k_9}\right),
\end{aligned}
\tag{8}
$$

$$D_{22} = \frac{1}{\mu}(\gamma_{\mathrm{H}} D_{13} + \gamma_{\mathrm{L}} D_{14} + \gamma_{\mathrm{A}} D_{15} + \gamma_{\mathrm{TH}} D_{16} + \gamma_{\mathrm{TL}} D_{17} + \gamma_{\mathrm{HH}} D_{18} + \gamma_{\mathrm{HL}} D_{19} + \gamma_{\mathrm{CH}} D_{20} + \gamma_{\mathrm{CL}} D_{21}).$$

Substituting (7) with (8) into the expressions for λ^{**} in (6) gives

$$\lambda^{**} = \frac{\beta\lambda^{**} S^{**}[1 + \frac{\xi(1-\epsilon)}{\mu+(1-\epsilon)\lambda^{**}}]G_1}{S^{**}\{1 + \frac{\xi}{\mu+(1-\epsilon)\lambda^{**}} + G_2[1 + \frac{\xi(1-\epsilon)}{\mu+(1-\epsilon)\lambda^{**}}]\lambda^{**}\}}, \tag{9}$$

where

$$G_1 = \frac{\theta_1}{k_2} + D_{11} + \theta_2 D_{12} + \theta_3 D_{13} + \theta_4 D_{14} + \theta_5 D_{15} + \theta_6 D_{16} + \theta_7 D_{17} + \theta_8 D_{18} + \theta_9 D_{19} + \theta_{10} D_{20} + \theta_{11} D_{21},$$

$$G_2 = \frac{1}{k_2} + D_{11} + D_{12} + D_{13} + D_{14} + D_{15} + D_{16} + D_{17} + D_{18} + D_{19} + D_{20} + D_{21} + D_{22},$$

so that the nonzero (endemic) equilibria of model (2) satisfy

$$Z_1\left(\lambda^{**}\right)^2 + Z_2\lambda^{**} + Z_3 = 0, \tag{10}$$

where

$$Z_1 = (1-\epsilon)G_2, \qquad Z_2 = G_2\left[\mu + \xi(1-\epsilon)\right] + (1-\epsilon)(1-\beta G_1) \quad \text{and} \quad Z_3 = k_1(1-\mathcal{R}_c). \tag{11}$$

The quadratic (10) can be analysed for the possibility of multiple endemic equilibria. It is worth noting that the coefficient Z_1 is always positive, and Z_3 is positive (negative) if $\mathcal{R}_c$ is less than (greater than) unity, respectively. Hence, the following result is established:

Theorem 2 *Model* (2) *has*

(i) *A unique endemic equilibrium if* $Z_3 < 0 \Leftrightarrow \mathcal{R}_c > 1$.
(ii) *A unique endemic equilibrium if* $Z_2 < 0$, *and* $Z_3 = 0$ *or* $Z_2^2 - 4Z_1Z_3 = 0$.
(iii) *Two endemic equilibria if* $Z_3 > 0$, $Z_2 < 0$ *and* $Z_2^2 - 4Z_1Z_3 > 0$.
(iv) *No endemic equilibrium otherwise.*

Case (iii) of Theorem 2 indicates the possibility of backward bifurcation in model (2) when $\mathcal{R}_c < 1$. To check for this, the discriminant $Z_2^2 - 4Z_1Z_3$ is set to zero, and the resulting equation is solved for the critical value of $\mathcal{R}_c$, giving

$$\mathcal{R}_c^c = 1 - \frac{Z_2^2}{4k_1Z_1},$$

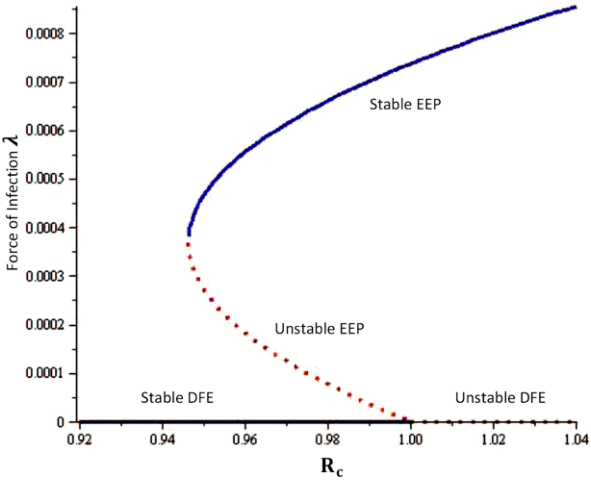

Fig. 2 Backward bifurcation diagram of model (2). Parameter values used are as given in Sect. 3.3

from which it can be shown that backward bifurcation occurs for values of $\mathcal{R}_c$ such that $0 < \mathcal{R}_c^c < \mathcal{R}_c < 1$. This phenomenon is illustrated by simulating model (2) with the following set of parameter values: $\Pi = 1\,100\,000/80 \times 365$, $\mu = 1/29\,500$, $\beta = 0.01$, $\delta_{\mathrm{HH}} = 0$, $\delta_{\mathrm{HL}} = 0$, $\delta_{\mathrm{CH}} = 1/2$, $\delta_{\mathrm{CL}} = 1/2$, $\xi = 0.06/100$, $\epsilon = 0.4$, $\alpha = 1/370$, $r = 0.999$, $f = 0.1$, $\kappa_{\mathrm{H}} = 0.1$, $\kappa_{\mathrm{L}} = 0.1$, $\tau_{\mathrm{H}} = 0.058$, $\tau_{\mathrm{L}} = 1$, $\gamma_{\mathrm{A}} = 1$, $\gamma_{\mathrm{TH}} = 3/700$, $\gamma_{\mathrm{TL}} = 1/800$, $\gamma_{\mathrm{HH}} = 3/800$, $\gamma_{\mathrm{HL}} = 1/8000$, $\gamma_{\mathrm{CH}} = 1/8000$, $\gamma_{\mathrm{CL}} = 1/9000$, $\psi_{\mathrm{H}} = 5.04$, $\psi_{\mathrm{L}} = 5.01$, $\phi_{\mathrm{H}} = 2.005$, $\phi_{\mathrm{L}} = 5.02$, $\sigma_{\mathrm{H}} = 5.075$, $\sigma_{\mathrm{L}} = 1.5$, $\theta_1 = 0.428$, $\theta_2 = 1$, $\theta_3 = 0.6$, $\theta_4 = 0.6$, $\theta_5 = 0.5$, $\theta_6 = 0.5$, $\theta_7 = 0.5$, $\theta_8 = 0.5$, $\theta_9 = 0.5$, $\theta_{10} = 0$, $\theta_{11} = 0$, $\gamma_{\mathrm{H}} = 1/8400$, $\gamma_{\mathrm{L}} = 1/8400$ (so that $\mathcal{R}_c = 0.983 < 1$ and $\mathcal{R}_c^c = 0.946$. Hence, $\mathcal{R}_c^c < \mathcal{R}_c < 1$). It should be mentioned, however, that the aforementioned parameter values may not all be realistic epidemiologically (the reader may refer to the study in Lipsitch and Murray (2003), and some of the references therein, for discussions on whether or not backward bifurcation can occur using a realistic set of parameter values).

The associated backward bifurcation diagram, depicted in Fig. 2, shows that the model has a disease-free equilibrium (corresponding to $\lambda^{**} = 0$) and two endemic equilibria (corresponding to $\lambda^{**} = 0.00067$ and $\lambda^{**} = 0.000062$); one of the endemic equilibria ($\lambda^{**} = 0.00067$) is LAS, the other ($\lambda^{**} = 0.000062$) is unstable (a saddle), and the disease-free equilibrium ($\mathcal{E}_0$) is LAS. This clearly shows the coexistence of two stable equilibria when $\mathcal{R}_c < 1$, confirming that the model exhibits backward bifurcation for $\mathcal{R}_c^c < \mathcal{R}_c < 1$. This result is summarized below for model (2) (a more rigorous proof of the backward bifurcation phenomenon of the model is given, using the centre manifold theory (Carr 1981), in Appendix A).

Theorem 3 *Model* (2) *exhibits backward bifurcation when Case* (iii) *of Theorem* 2 *holds and* $\mathcal{R}_c^c < \mathcal{R}_c < 1$.

The epidemiological implication of the aforementioned backward bifurcation phenomenon is that having the reproduction threshold ($\mathcal{R}_c$) less than unity, while necessary, is not sufficient for the effective control or elimination of the H1N1 pandemic

from the community (since two stable attractors coexist when $\mathcal{R}_c^c < \mathcal{R}_c < 1$). In such a case, effective disease control or elimination when $\mathcal{R}_c^c < \mathcal{R}_c < 1$ is dependent on the initial sizes of the subpopulations of the model (see Elbasha and Gumel 2006; Sharomi et al. 2007 for further discussion on the epidemiological consequences of backward bifurcation).

Numerical simulation results, depicted in Fig. 3A, suggest that the unique endemic equilibrium guaranteed by Items (i) and (ii) of Theorem 2 is LAS when it exists.

3.4 Effect of Perfect Vaccine on Backward Bifurcation

Consider model (2) with a perfect H1N1 vaccine (that is, $\epsilon = 1$). In such a case, the associated reproduction number is $\tilde{\mathcal{R}}_c = \mathcal{R}_c|_{\epsilon=1}$. It follows from (11) that if $\epsilon = 1$, the coefficients $Z_1 = 0$ and $Z_2 > 0$, so that the quadratic (10) reduces to a linear equation in λ^{**} (with $\lambda^{**} = -Z_3/Z_2$). In this case, model (2) has a unique endemic equilibrium if $Z_3 < 0$ (i.e., $\tilde{\mathcal{R}}_c > 1$), ruling out backward bifurcation in the model for this case (since no two endemic equilibria exist when $\tilde{\mathcal{R}}_c < 1$. The presence of two endemic equilibria when $\tilde{\mathcal{R}}_c < 1$ is a necessary requirement for the existence of backward bifurcation). Furthermore, it follows that $Z_3 = 0$ when $\tilde{\mathcal{R}}_c = 1$. Thus, in such a case (with $Z_1 = Z_3 = 0$), the quadratic (10) has only the trivial solution $\lambda^{**} = 0$ (which corresponds to the DFE, $\mathcal{E}_0$). This result is summarized below.

Lemma 3 *Consider the case where the vaccine is perfect* ($\epsilon = 1$). *Model* (2) *has a unique endemic equilibrium whenever* $\tilde{\mathcal{R}}_c > 1$, *and no endemic equilibrium otherwise*.

To further confirm the impossibility of backward bifurcation occurring when the vaccine is perfect, a global asymptotic stability proof of the DFE is given for this case ($\epsilon = 1$) below.

3.4.1 Global Stability of DFE of the Model with $\epsilon = 1$

Consider model (2) with a perfect vaccine (i.e., $\epsilon = 1$). We claim the following:

Theorem 4 *The DFE of model* (2) *with* $\epsilon = 1$ *is globally asymptotically stable whenever* $\tilde{\mathcal{R}}_c \leq \frac{\mu}{k_1} < 1$.

Proof Consider model (2) with $\epsilon = 1$. Further, consider the Lyapunov function

$$\begin{aligned}\mathcal{F} = {} & a_1 L + a_2 I_1 + a_3 Y_1 + a_4 I_2 + a_5 Y_2 + a_6 A + a_7 T_{\mathrm{H}} + a_8 T_{\mathrm{L}} \\ & + a_9 H_{\mathrm{H}} + a_{10} H_{\mathrm{L}} + a_{11} C_{\mathrm{H}} + a_{12} C_{\mathrm{L}}\end{aligned}$$

with

$$a_1 = \frac{k_2 k_3 k_4 k_5 k_6 k_7 k_8 k_9 k_{10} k_{11} k_{12} k_{13} N^* \tilde{\mathcal{R}}_c}{S^* \beta},$$

$$
\begin{aligned}
a_2 &= k_2k_4k_6k_7k_9k_{11}k_{13}\big[k_{10}k_{12}(k_5k_8+\theta_3\kappa_{\mathrm{H}}k_8+\theta_6\tau_{\mathrm{H}}k_5)\\
&\qquad +(\psi_{\mathrm{H}}\kappa_{\mathrm{H}}k_8+\phi_{\mathrm{H}}\tau_{\mathrm{H}}k_5)(\theta_8k_{12}+\theta_{10}\sigma_{\mathrm{H}})\big],\\
a_3 &= k_2k_3k_5k_7k_8k_{10}k_{12}\big[k_{11}k_{13}(\theta_2k_6k_9+\theta_4\kappa_{\mathrm{L}}k_9+\theta_7\tau_{\mathrm{L}}k_6)\\
&\qquad +(\psi_{\mathrm{L}}\kappa_{\mathrm{L}}k_9+\phi_{\mathrm{L}}\tau_{\mathrm{L}}k_6)(\theta_9k_{13}+\theta_{11}\sigma_{\mathrm{L}})\big],\\
a_4 &= k_2k_3k_4k_6k_7k_8k_9k_{11}k_{13}(\theta_3k_{10}k_{12}+\theta_8\psi_{\mathrm{H}}k_{12}+\theta_{10}\sigma_{\mathrm{H}}\psi_{\mathrm{H}}),\\
a_5 &= k_2k_3k_4k_5k_7k_8k_9k_{10}k_{12}(\theta_4k_{11}k_{13}+\theta_9\psi_{\mathrm{L}}k_{13}+\theta_{11}\sigma_{\mathrm{L}}\psi_{\mathrm{L}}),\\
a_6 &= \theta_5k_2k_3k_4k_5k_6k_8k_9k_{10}k_{11}k_{12}k_{13},\\
a_7 &= k_2k_3k_4k_5k_6k_7k_9k_{11}k_{13}(\theta_6k_{10}k_{12}+\theta_8\phi_{\mathrm{H}}k_{12}+\theta_{10}\sigma_{\mathrm{H}}\phi_{\mathrm{H}}),\\
a_8 &= k_2k_3k_4k_5k_6k_7k_8k_{10}k_{12}(\theta_7k_{11}k_{13}+\theta_9\phi_{\mathrm{L}}k_{13}+\theta_{11}\sigma_{\mathrm{L}}\phi_{\mathrm{L}}),\\
a_9 &= k_2k_3k_4k_5k_6k_7k_8k_9k_{11}k_{13}(\theta_8k_{12}+\theta_{10}\sigma_{\mathrm{H}}),\\
a_{10} &= k_2k_3k_4k_5k_6k_7k_8k_9k_{10}k_{12}(\theta_9k_{13}+\theta_{11}\sigma_{\mathrm{L}}),\\
a_{11} &= \theta_{10}k_2k_3k_4k_5k_6k_7k_8k_9k_{10}k_{11}k_{13},\\
a_{12} &= \theta_{11}k_2k_3k_4k_5k_6k_7k_8k_9k_{10}k_{11}k_{12},
\end{aligned}
$$

so that (where a dot represents differentiation with respect to t)

$$
\begin{aligned}
\dot{\mathcal{F}} &= a_1\dot{L}+a_2\dot{I}_1+a_3\dot{Y}_1+a_4\dot{I}_2+a_5\dot{Y}_2+a_6\dot{A}+a_7\dot{T}_{\mathrm{H}}+a_8\dot{T}_{\mathrm{L}}\\
&\quad +a_9\dot{H}_{\mathrm{H}}+a_{10}\dot{H}_{\mathrm{L}}+a_{11}\dot{C}_{\mathrm{H}}+a_{12}\dot{C}_{\mathrm{L}}\\
&= \frac{k_2k_3k_4k_5k_6k_7k_8k_9k_{10}k_{11}k_{12}k_{13}SN^*\lambda\tilde{\mathcal{R}}_c}{S^*\beta}\\
&\quad -\frac{k_2^2k_3k_4k_5k_6k_7k_8k_9k_{10}k_{11}k_{12}k_{13}N^*L\tilde{\mathcal{R}}_c}{S^*\beta}\\
&\quad -\frac{k_2k_3k_4k_5k_6k_7k_8k_9k_{10}k_{11}k_{12}k_{13}N\lambda}{\beta}+\frac{k_2^2k_3k_4k_5k_6k_7k_8k_9k_{10}k_{11}k_{12}k_{13}N^*L\tilde{\mathcal{R}}_c}{S^*\beta}\\
&= \frac{k_2k_3k_4k_5k_6k_7k_8k_9k_{10}k_{11}k_{12}k_{13}SN^*\lambda\tilde{\mathcal{R}}_c}{S^*\beta}-\frac{k_2k_3k_4k_5k_6k_7k_8k_9k_{10}k_{11}k_{12}k_{13}N\lambda}{\beta}\\
&= \frac{k_2k_3k_4k_5k_6k_7k_8k_9k_{10}k_{11}k_{12}k_{13}N\lambda}{\beta}\left(\frac{SN^*\tilde{\mathcal{R}}_c}{S^*N}-1\right)\\
&= \frac{k_2k_3k_4k_5k_6k_7k_8k_9k_{10}k_{11}k_{12}k_{13}N\lambda}{\beta}\left(\frac{Sk_1\tilde{\mathcal{R}}_c}{N\mu}-1\right)\\
&\le \frac{k_2k_3k_4k_5k_6k_7k_8k_9k_{10}k_{11}k_{12}k_{13}N\lambda}{\beta}\left(\frac{k_1\tilde{\mathcal{R}}_c}{\mu}-1\right)\quad \text{since } S\le N \text{ in } \mathcal{D}\\
&\le 0\quad \text{for } \tilde{\mathcal{R}}_c\le\frac{\mu}{k_1}<1.
\end{aligned}
$$

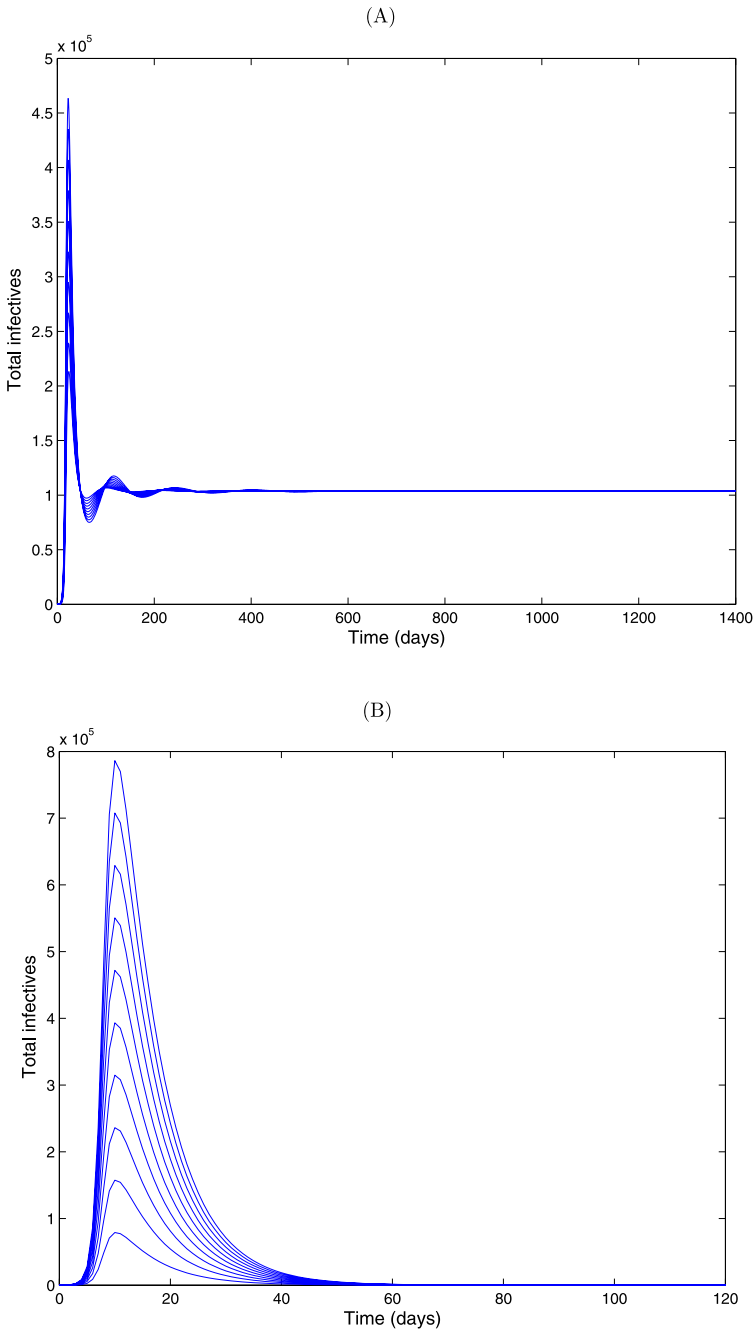

Fig. 3 Solutions profile of the total number of infections as a function of time for the case **A** $\xi = 0.5$, $\epsilon = 0.6$, $\beta = 2.7$ and $\Pi = 1\,100\,000/80$ (so that $\mathcal{R}_c = 5.292 > 1$); **B** $\epsilon = 1, \xi = 0.001$ and $\beta = 2.7$ (so that $\tilde{\mathcal{R}}_c = 0.4380 < 1$). Other parameter values used are as given in Table 2

Thus, $\dot{\mathcal{F}} \leq 0$ if $\tilde{\mathcal{R}}_c \leq \frac{\mu}{k_1}$ with $\dot{\mathcal{F}} = 0$ if and only if $L = I_1 = Y_1 = I_2 = Y_2 = A = T_{\mathrm{H}} = T_{\mathrm{L}} = H_{\mathrm{H}} = H_{\mathrm{L}} = C_{\mathrm{H}} = C_{\mathrm{L}} = 0$. It follows, from the Lasalle's Invariance Principle (Hale 1969) that $L \to 0$, $I_1 \to 0$, $Y_1 \to 0$, $I_2 \to 0$, $Y_2 \to 0$, $A \to 0$, $T_{\mathrm{H}} \to 0$, $T_{\mathrm{L}} \to 0$, $H_{\mathrm{H}} \to 0$, $H_{\mathrm{L}} \to 0$, $C_{\mathrm{H}} \to 0$ and $C_{\mathrm{L}} \to 0$ as $t \to \infty$. Substituting $(L, I_1, Y_1, I_2, Y_2, A, T_{\mathrm{H}}, T_{\mathrm{L}}, H_{\mathrm{H}}, H_{\mathrm{L}}, C_{\mathrm{H}}, C_{\mathrm{L}}) = (0, 0, 0, 0, 0, 0, 0, 0, 0, 0, 0, 0)$ into the first two equations of the model shows, respectively, that $S \to \frac{\Pi}{k_1}$ and $V \to \frac{\xi \Pi}{\mu k_1}$ as $t \to \infty$. Thus, $(S, V, L, I_1, Y_1, I_2, Y_2, A, T_{\mathrm{H}}, T_{\mathrm{L}}, H_{\mathrm{H}}, H_{\mathrm{L}}, C_{\mathrm{H}}, C_{\mathrm{L}}) \to (\frac{\Pi}{k_1}, \frac{\xi \Pi}{\mu k_1}, 0, 0, 0, 0, 0, 0, 0, 0, 0, 0, 0, 0)$ as $t \to \infty$ for $\tilde{\mathcal{R}}_c \leq \frac{\mu}{k_1} < 1$ and $\epsilon = 1$. Further, since $\mathcal{D}$ is positively invariant, it follows that the DFE, $\mathcal{E}_0$, is GAS in $\mathcal{D}$ for all nonnegative initial conditions of the state variables of model (2) if $\tilde{\mathcal{R}}_c \leq \frac{\mu}{k_1} < 1$ and $\epsilon = 1$. □

Figure 3B depicts the total number of infections as a function of time for the case with $\epsilon = 1$ and $\tilde{\mathcal{R}}_c < 1$, showing convergence to the DFE (in line with Theorem 4). It is worth stating that further extensive numerical simulations suggest that the condition $\tilde{\mathcal{R}}_c < \mu/k_1$ is only sufficient, but not necessary, for disease elimination when $\tilde{\mathcal{R}}_c < 1$ (for $\epsilon = 1$), since the solutions converge to the DFE even for $\mu/k_1 < \tilde{\mathcal{R}}_c < 1$.

In summary, it is clear from Theorems 3 and 4 that the backward bifurcation phenomenon of the model is caused by the imperfect nature of the H1N1 vaccine (i.e., $0 < \epsilon < 1$). Furthermore, a perfect vaccine ($\epsilon = 1$) will lead to the elimination of the disease if the reproduction threshold quantity $\tilde{\mathcal{R}}_c$ is brought to (and maintained at) a value less than $\frac{\mu}{k_1}$. In other words, in the case where the H1N1 vaccine is perfect, the classical epidemiological requirement of having the reproduction threshold less than unity (that is, $\tilde{\mathcal{R}}_c \leq \frac{\mu}{k_1} < 1$) is necessary and sufficient for H1N1 elimination from the community. Thus, this study emphasizes the pressing need for the design of perfect vaccines to handle emerging diseases, such as H1N1.

4 Numerical Simulations

Model (2) is simulated using the parameter values given in Table 2 (unless otherwise stated) and appropriate demographic (initial) data for the province of Manitoba, to evaluate various anti-H1N1 intervention scenarios. The simulations were carried out using MATLAB software. Simulations of the model for the first wave of the pandemic in Manitoba, which occurred during the period April 29–July 29, 2009, suggest a cumulative mortality of 10 people, over 200 hospitalizations, about 45 000 latent cases and 45 people admitted to ICU (Fig. 4). These simulations, which correspond to a reproduction number $\mathcal{R}_c = 1.3227$ (Fraser et al. 2009; Nishiura et al. 2009), are consistent with the observed data for the province of Manitoba. Having validated the model in this way, it is then reasonable to use the model to explore various scenarios for the second wave of H1N1 (which is currently underway) for the province of Manitoba.

It is assumed that the second wave of the H1N1 pandemic started early in October 2009, and the corresponding reproduction number is $\mathcal{R}_c = 1.9106$ (to account for the assumption that the second wave of a pandemic is known to be more severe than the

Table 2 Parameter values used in the simulations

Parameter	Nominal values	Ranges	References
Π	$\frac{1100000}{80\times365}$/day		(Statistics Canada 2009a)
β	0.27	0.27–0.39/day	
$1/\mu$	80×365 days	77–82 years	(Statistics Canada 2009b)
δ_{HH}	0		assumed
δ_{HL}	0		assumed
δ_{CH}	1/4		estimated
δ_{CL}	1/6		estimated
ξ	35/100		estimated
ϵ	0.8		(Demicheli et al. 2009)
$1/\alpha$	7	1–7 days	(Centers for Disease Control and Prevention 2009e)
r	0.4	[0,1]	assumed
f	0.6	[0,1]	assumed
κ_H	0.6		
κ_L	0.3		
τ_H	0.06		estimated
τ_L	0.04		estimated
γ_H	$1-\phi_H$		
γ_L	$1-\phi_L$		
γ_A	1		estimated
γ_{TH}	3/20		estimated
γ_{TL}	1/10		estimated
γ_{HH}	3/8		estimated
γ_{HL}	1/4		estimated
γ_{CH}	3/42		estimated
γ_{CL}	1/21		Winnipeg Regional Health Authority
ψ_H	0.04		Winnipeg Regional Health Authority
ψ_L	0.01		(World Health Organization 2009e)
ϕ_H	0.02		Winnipeg Regional Health Authority
ϕ_L	0.005		Winnipeg Regional Health Authority
σ_H	0.075		assumed
σ_L	0.05		assumed
θ_1	0.5	[0,1)	assumed
θ_2	1		
θ_3	0.5	[0,1)	assumed
θ_4	0.5	[0,1)	assumed
θ_5	0.3	[0,1)	assumed
θ_6	0.3	[0,1)	assumed
θ_7	0.3	[0,1)	assumed
θ_8	0.045	[0,1)	assumed
θ_9	0.045	[0,1)	assumed
θ_{10}	0	[0,1)	assumed
θ_{11}	0	[0,1)	assumed

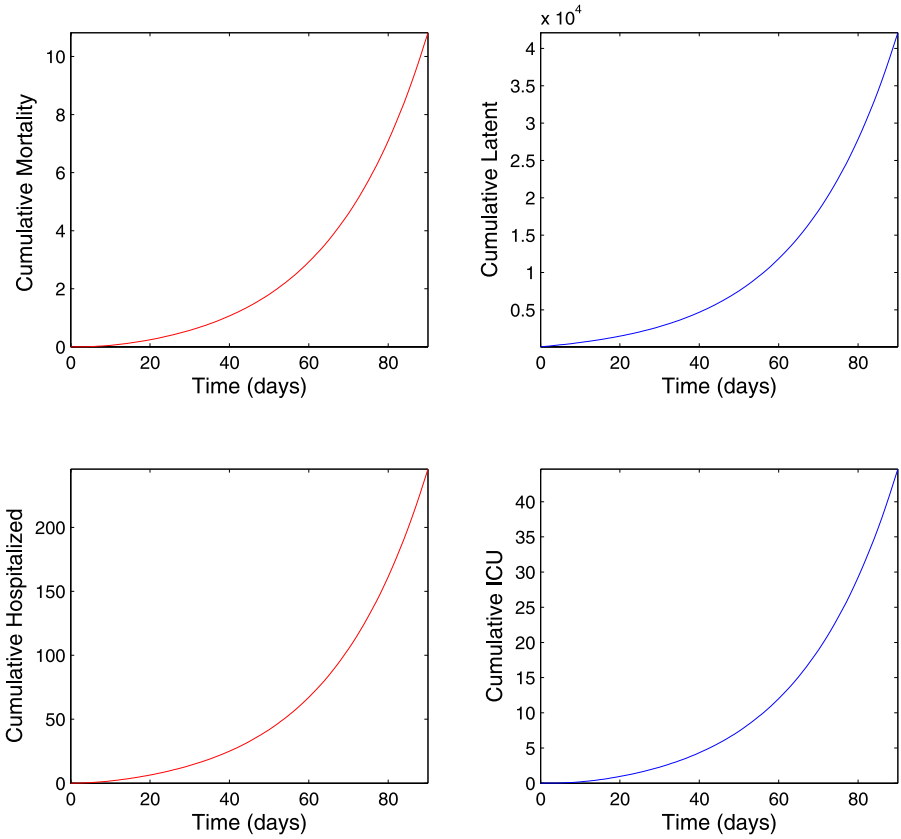

Fig. 4 Simulations of the first wave, for the province of Manitoba, giving the cumulative numbers of latent cases, H1N1-induced mortality, hospitalizations (not in ICU) and ICU admissions. Parameter values used are as given in Table 2 (so that $\mathcal{R}_c = 1.3227$)

first wave). Although it is assumed that mass vaccination commences on October 26, 2009 in Manitoba, it is further assumed that the full vaccine effect (in reducing disease burden) is not felt in the community until at least after the first week of November. This is to account for the fact that, at individual level, protective level of antibodies is not achieved in vaccinated individuals until 2–3 weeks following the administration of the vaccine. Furthermore, at the population level, a few weeks are probably needed before a significant proportion of the population is vaccinated, even when mass vaccination clinics are used. These facts are incorporated in the simulations by including a time lag after which the full vaccine effect is felt in the community (Cox et al. 2008; Greenberg et al. 2009).

A contour plot of the reproduction number ($\mathcal{R}_c$), as a function of the vaccine efficacy and fraction of individuals vaccinated at steady state, is depicted in Fig. 5. It follows from this figure that with the assumed vaccine efficacy of 80%, at least 60% of Manitobans need to be vaccinated in order for effective control or elimination of the second wave of H1N1 in Manitoba to be feasible (it should be recalled

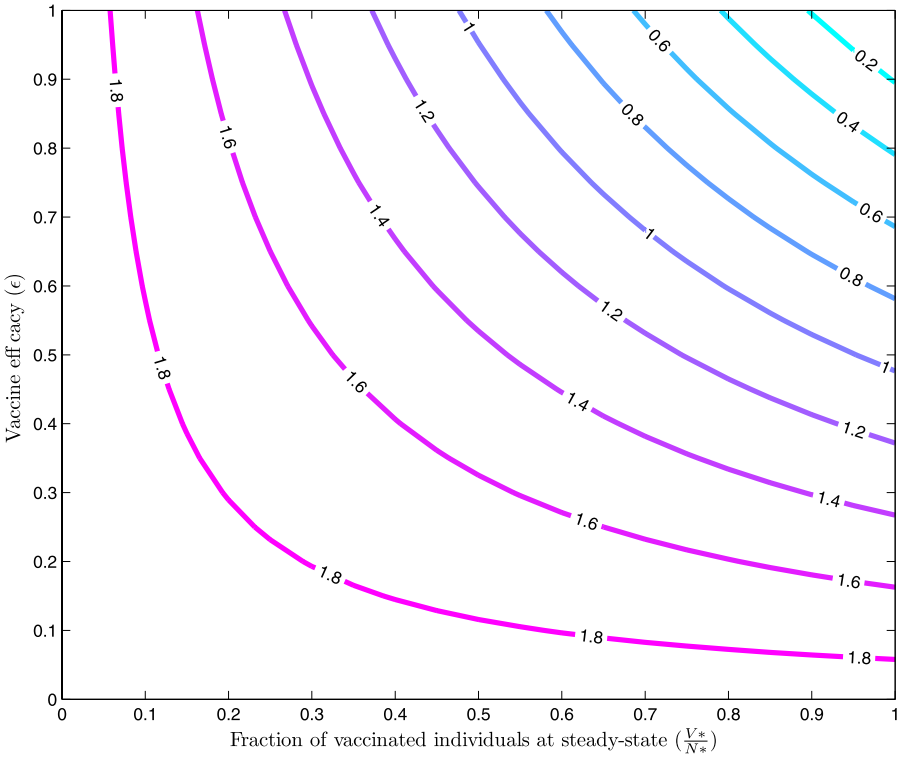

Fig. 5 Contour plot of the reproduction number ($\mathcal{R}_c$) as a function of vaccine efficacy (ϵ) and fraction of susceptible individuals vaccinated at steady state ($\frac{V^*}{N^*}$). Parameter values used are as given in Table 2

that, although this combination of efficacy and coverage rate guarantees that the reproduction threshold $\mathcal{R}_c$ is less than unity, the phenomenon of backward bifurcation in the model when $\mathcal{R}_c^c < \mathcal{R}_c < 1$ makes the classical epidemiological requirement, $\mathcal{R}_c < 1$, necessary but not sufficient for effective disease control or elimination. In other words, for an imperfect vaccine, the reproduction threshold, $\mathcal{R}_c$, has to be brought to a value less than $\mathcal{R}_c^c$ for disease elimination to be guaranteed, owing to the phenomenon of backward bifurcation).

Figure 6A depicts a time series plot of the number of hospitalized individuals, for the case where 10% of the total Manitoban population are assumed to have preexisting (infection-acquired) immunity (due to the first wave), for various time periods when the vaccine impact is expected to take effect. It is evident from this figure that the peak, which is projected to occur at the end of November or early in December, increases with increasing duration of time before the vaccine impact is felt. Furthermore, the figure shows that the H1N1 pandemic would run until late January or early February 2010. Similar plots are depicted for the ICU admissions (Fig. 6B) and H1N1-induced mortality (Fig. 6C). The associated cumulative numbers of hospitalized, ICU admissions and mortality are given in Table 3.

For the case where the assumed preexisting immunity is 20%, the model shows a milder pandemic compared to the case where the preexisting immunity is assumed to

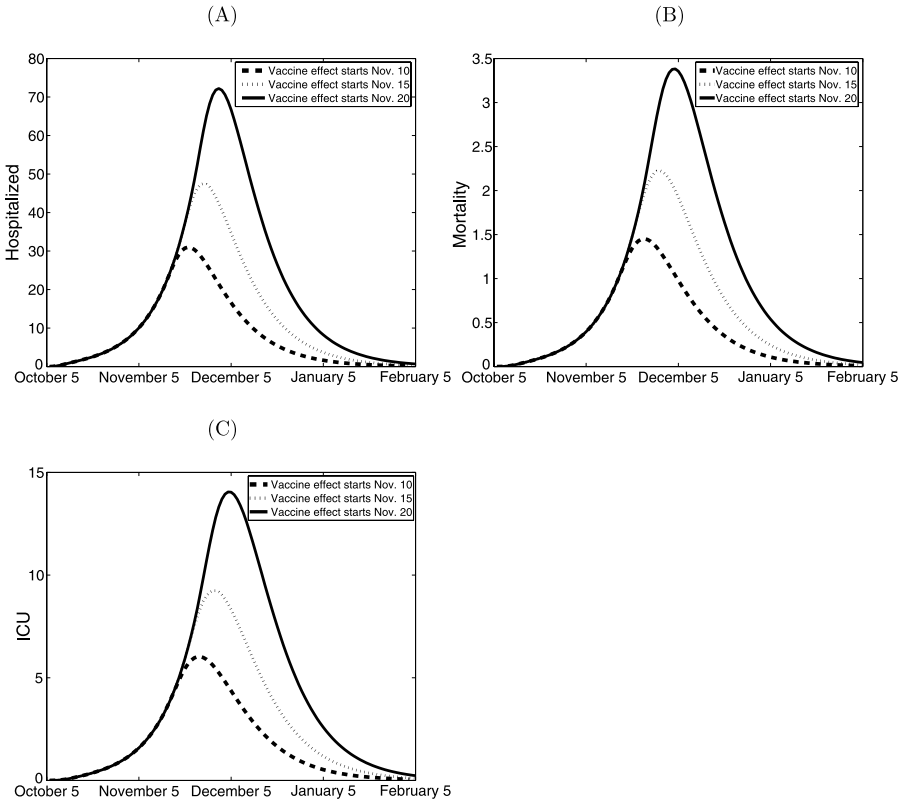

Fig. 6 Time series plot for **A** Hospitalization, **B** H1N1-induced mortality, **C** ICU admissions, corresponding to different times when the vaccine effect is felt in the community, for the case where 10% of the population have preexisting immunity. Parameter values used are as given in Table 2

Table 3 Summary of disease burden for the second wave corresponding to the case where 10% of the population have preexisting immunity

Number	Vaccine Effect Starts		
	November 10	November 15	November 20
Cumulative Hospitalized	946	1462	2233
Cumulative ICU	194	300	459
Cumulative Mortality	45	70	108

be 10% (Figs. 7A–7C; see also Table 4). It is clear from Table 3 that, with 10% preexisting population-wide immunity, the province of Manitoba could have between 946–2223 hospitalizations, 194–459 ICU cases and 45–108 H1N1-induced mortality, depending on when the vaccine impact takes effect in the community. Similarly, it follows from Table 4 that, for the case where 20% of the populace have prior immunity, the province could have: 436–849 hospitalizations, 90–175 ICU admissions

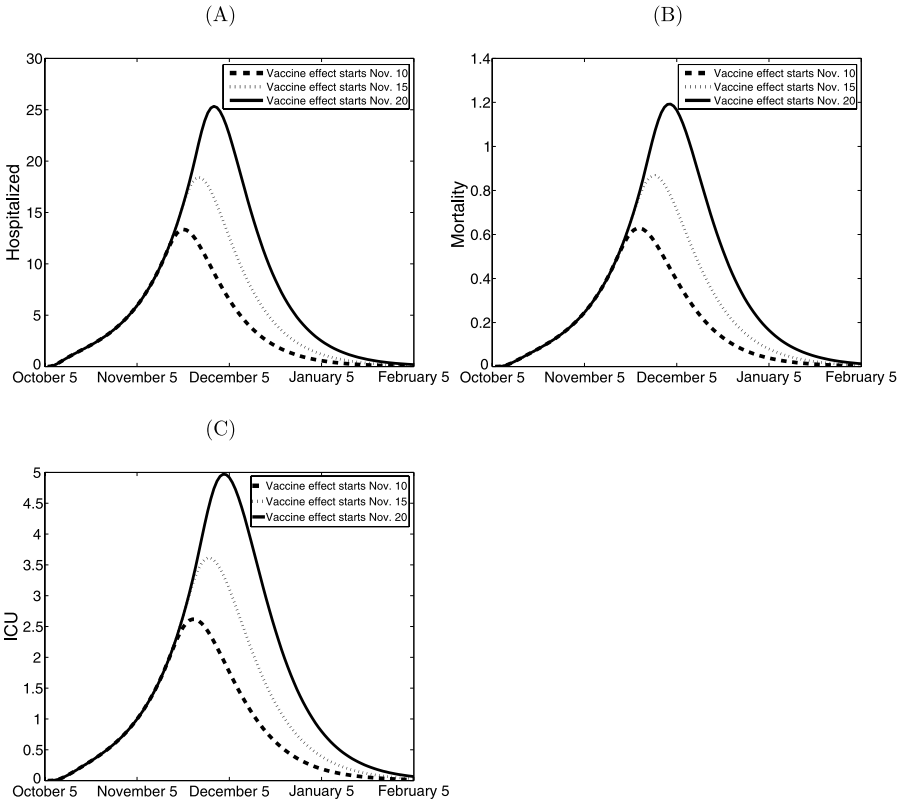

Fig. 7 Time series plot for **A** Hospitalization, **B** H1N1-induced mortality, **C** ICU admissions, corresponding to different times when the vaccine effect is felt in the community, for the case where 20% of the population have preexisting immunity. Parameter values used are as given in Table 2

Table 4 Summary of disease burden for the second wave corresponding to the case where 20% of the population have preexisting immunity

Number	Vaccine Effect Starts		
	November 10	November 15	November 20
Cumulative Hospitalized	436	611	849
Cumulative ICU	90	126	175
Cumulative Mortality	21	30	41

and 21–41 deaths. In summary, these results show that the timely implementation of a vaccination program, coupled with the proportion of individuals with preexisting immunity, are crucial to the expected burden of the H1N1 pandemic in the province of Manitoba. Further, these simulations suggest that the burden of the second wave would be at least three times that of the first wave.

5 Conclusions

A deterministic compartmental model for the transmission dynamics of the influenza H1N1 pandemic, which subdivides the infected population in terms of their risk of developing severe illness, is designed and rigorously analysed to gain insight into its dynamical features. Simulations were carried out using partial data from the province of Manitoba, Canada. The theoretical analysis of the model showed the following:

(i) The model exhibits the phenomenon of backward bifurcation, where a stable disease-free equilibrium coexists with a stable endemic equilibrium when the associated reproduction threshold is less than unity. The phenomenon of backward bifurcation is caused by the imperfect nature of the H1N1 vaccine.
(ii) The model with perfect vaccine (with efficacy 100%) is shown to have a globally asymptotically stable DFE whenever the associated reproduction threshold is less than unity and a unique endemic equilibrium when the threshold exceeds unity. Thus, this study shows that the vaccine-induced backward bifurcation exhibited by the model can be removed if the vaccine is 100% effective.
(iii) The model has a unique endemic equilibrium when the associated reproduction threshold exceeds unity.

Numerical simulations of the model, using relevant epidemiological and demographic data for the province of Manitoba, suggest the following:

(a) The timely implementation of a mass vaccination program, together with the percentage of the Manitoban population with preexisting (infection-acquired) immunity, is crucial to the expected burden of the second wave of the H1N1 pandemic.
(b) With the estimated vaccine efficacy of 80%, at least 60% of Manitobans need to be vaccinated in order for the effective control or elimination of the H1N1 pandemic to be feasible.
(c) The burden of the second wave of the H1N1 pandemic is expected to be at least three times that of the first wave; and the second wave would last until the early part of 2010.

It is worth emphasizing that the simulation results reported above are, of course, sensitive to changes in the parameter and initial values (the model developed here is, however, robust enough to allow for more realistic estimation of the pandemic H1N1 burden as more data becomes available).

Acknowledgements ABG acknowledges, with thanks, the support in part of the Natural Science and Engineering Research Council (NSERC) and Mathematics of Information Technology and Complex Systems (MITACS) of Canada. CNP acknowledges the support of the Manitoba Health Research Council Scholarship. OS gratefully acknowledges the support the University of Manitoba Graduate Fellowship. The authors are grateful to the anonymous reviewers for their constructive comments.

Appendix A: Proof of Theorem 3

Proof The centre manifold theory (Carr 1981), as described in Castillo-Chavez and Song (2004) (Theorem 4.1), will be used to establish the backward bifurcation of the model (see also Feng et al. 2000; Podder and Gumel 2009; Sharomi

et al. 2008). To apply this theory, the following simplification and change of variables are made first of all. Let $S = x_1, V = x_2, L = x_3, I_1 = x_4, Y_1 = x_5, I_2 = x_6, Y_2 = x_7, A = x_8, T_{\mathrm{H}} = x_9, T_{\mathrm{L}} = x_{10}, H_{\mathrm{H}} = x_{11}, H_{\mathrm{L}} = x_{12}, C_{\mathrm{H}} = x_{13}, C_{\mathrm{L}} = x_{14}$, and $R = x_{15}$, so that $N = x_1 + x_2 + x_3 + x_4 + x_5 + x_6 + x_7 + x_8 + x_9 + x_{10} + x_{11} + x_{12} + x_{13} + x_{14} + x_{15}$. Further, by using the vector notation $X = (x_1, x_2, x_3, x_4, x_5, x_6, x_7, x_8, x_9, x_{10}, x_{11}, x_{12}, x_{13}, x_{14}, x_{15})^{\mathrm{T}}$, model (2) can be written in the form $\frac{dX}{dt} = (f_1, f_2, f_3, f_4, f_5, f_6, f_7, f_8, f_9, f_{10}, f_{11}, f_{12}, f_{13}, f_{14}, f_{15})^{\mathrm{T}}$ as follows:

$$
\begin{aligned}
\frac{dx_1}{dt} &= \Pi - \lambda x_1 - k_1 x_1,\\
\frac{dx_2}{dt} &= \xi x_1 - (1-\epsilon)\lambda x_2 - \mu x_2,\\
\frac{dx_3}{dt} &= \lambda x_1 + (1-\epsilon)\lambda x_2 - k_2 x_3,\\
\frac{dx_4}{dt} &= f r \alpha x_3 - k_3 x_4,\\
\frac{dx_5}{dt} &= (1-f) r \alpha x_3 - k_4 x_5,\\
\frac{dx_6}{dt} &= \kappa_{\mathrm{H}} x_4 - k_5 x_6,\\
\frac{dx_7}{dt} &= \kappa_{\mathrm{L}} x_5 - k_6 x_7,\\
\frac{dx_8}{dt} &= (1-r)\alpha x_3 - k_7 x_8,\\
\frac{dx_9}{dt} &= \tau_{\mathrm{H}} x_4 - k_8 x_9,\\
\frac{dx_{10}}{dt} &= \tau_{\mathrm{L}} x_5 - k_9 x_{10},\\
\frac{dx_{11}}{dt} &= psi_{\mathrm{H}} x_6 + \phi_{\mathrm{H}} x_9 - k_{10} x_{11},\\
\frac{dx_{12}}{dt} &= \psi_{\mathrm{L}} x_7 + \phi_{\mathrm{L}} x_{10} - k_{11} x_{12},\\
\frac{dx_{13}}{dt} &= \sigma_{\mathrm{H}} x_{11} - k_{12} x_{13},\\
\frac{dx_{14}}{dt} &= \sigma_{\mathrm{L}} x_{12} - k_{13} x_{14}, n\\
\frac{dx_{15}}{dt} &= \gamma_{\mathrm{H}} x_6 + \gamma_{\mathrm{L}} x_7 + \gamma_{\mathrm{A}} x_8 + \gamma_{\mathrm{TH}} x_9 + \gamma_{\mathrm{TL}} x_{10}\\
&\quad + \gamma_{\mathrm{HH}} x_{11} + \gamma_{\mathrm{HL}} x_{12} + \gamma_{\mathrm{CH}} x_{13} + \gamma_{\mathrm{CL}} x_{14} - \mu x_{15},
\end{aligned}
\tag{12}
$$

with

$$\lambda = \frac{\beta(Q_1 + Q_2)}{N}, \tag{13}$$

where

$$Q_1 = \theta_1 x_3 + x_4 + \theta_2 x_5 + \theta_3 x_6 + \theta_4 x_7 + \theta_5 x_8 + \theta_6 x_9,$$

$$Q_2 = \theta_7 x_{10} + \theta_8 x_{11} + \theta_9 x_{12} + \theta_{10} x_{13} + \theta_{11} x_{14}.$$

The Jacobian of system (12), at $\mathcal{E}_0$, is given by

$$J(\mathcal{E}_0) = \begin{bmatrix} J_1 & J_2 \\ J_3 & J_4 \end{bmatrix}$$

with

$$J_1 = \begin{bmatrix} -k_1 & 0 & -\frac{\beta\theta_1\mu}{k_1} & -\frac{\beta\mu}{k_1} & -\frac{\beta\theta_2\mu}{k_1} & -\frac{\beta\theta_3\mu}{k_1} & -\frac{\beta\theta_4\mu}{k_1} \\ \xi & -\mu & -\frac{\beta\theta_1\xi(1-\epsilon)}{k_1} & -\frac{\beta\xi(1-\epsilon)}{k_1} & -\frac{\beta\theta_2\xi(1-\epsilon)}{k_1} & -\frac{\beta\theta_3\xi(1-\epsilon)}{k_1} & -\frac{\beta\theta_4\xi(1-\epsilon)}{k_1} \\ 0 & 0 & \frac{\beta\theta_1\gamma_1}{k_1} - k_2 & \frac{\beta\gamma_1}{k_1} & \frac{\beta\theta_2\gamma_1}{k_1} & \frac{\beta\theta_3\gamma_1}{k_1} & \frac{\beta\theta_4\gamma_1}{k_1} \\ 0 & 0 & fr\alpha & -k_3 & 0 & 0 & 0 \\ 0 & 0 & (1-f)r\alpha & 0 & -k_4 & 0 & 0 \\ 0 & 0 & 0 & \kappa_{\mathrm{H}} & 0 & -k_5 & 0 \\ 0 & 0 & 0 & 0 & \kappa_{\mathrm{L}} & 0 & -k_6 \end{bmatrix},$$

$$J_2 = \begin{bmatrix} -\frac{\beta\theta_5\mu}{k_1} & -\frac{\beta\theta_6\mu}{k_1} & -\frac{\beta\theta_7\mu}{k_1} & -\frac{\beta\theta_8\mu}{k_1} & -\frac{\beta\theta_9\mu}{k_1} & -\frac{\beta\theta_{10}\mu}{k_1} & -\frac{\beta\theta_{11}\mu}{k_1} & 0 \\ -\frac{\beta\theta_5\xi(1-\epsilon)}{k_1} & -\frac{\beta\theta_6\xi(1-\epsilon)}{k_1} & -\frac{\beta\theta_7\xi(1-\epsilon)}{k_1} & -\frac{\beta\theta_8\xi(1-\epsilon)}{k_1} & -\frac{\beta\theta_9\xi(1-\epsilon)}{k_1} & -\frac{\beta\theta_{10}\xi(1-\epsilon)}{k_1} & -\frac{\beta\theta_{11}\xi(1-\epsilon)}{k_1} & 0 \\ \frac{\beta\theta_5\gamma_1}{k_1} & \frac{\beta\theta_6\gamma_1}{k_1} & \frac{\beta\theta_7\gamma_1}{k_1} & \frac{\beta\theta_8\gamma_1}{k_1} & \frac{\beta\theta_9\gamma_1}{k_1} & \frac{\beta\theta_{10}\gamma_1}{k_1} & \frac{\beta\theta_{11}\gamma_1}{k_1} & 0 \\ 0 & 0 & 0 & 0 & 0 & 0 & 0 & 0 \\ 0 & 0 & 0 & 0 & 0 & 0 & 0 & 0 \\ 0 & 0 & 0 & 0 & 0 & 0 & 0 & 0 \\ 0 & 0 & 0 & 0 & 0 & 0 & 0 & 0 \end{bmatrix},$$

$$J_3 = \begin{bmatrix} 0 & 0 & (1-r)\alpha & 0 & 0 & 0 & 0 \\ 0 & 0 & 0 & \tau_{\mathrm{H}} & 0 & 0 & 0 \\ 0 & 0 & 0 & 0 & \tau_{\mathrm{L}} & 0 & 0 \\ 0 & 0 & 0 & 0 & 0 & \psi_{\mathrm{H}} & 0 \\ 0 & 0 & 0 & 0 & 0 & 0 & \psi_{\mathrm{L}} \\ 0 & 0 & 0 & 0 & 0 & 0 & 0 \\ 0 & 0 & 0 & 0 & 0 & 0 & 0 \\ 0 & 0 & 0 & 0 & 0 & \gamma_{\mathrm{H}} & \gamma_{\mathrm{L}} \end{bmatrix},$$

$$J_4 = \begin{bmatrix} -k_7 & 0 & 0 & 0 & 0 & 0 & 0 & 0 \\ 0 & -k_8 & 0 & 0 & 0 & 0 & 0 & 0 \\ 0 & 0 & -k_9 & 0 & 0 & 0 & 0 & 0 \\ 0 & \phi_{\mathrm{H}} & 0 & -k_{10} & 0 & 0 & 0 & 0 \\ 0 & 0 & \phi_{\mathrm{L}} & 0 & -k_{11} & 0 & 0 & 0 \\ 0 & 0 & 0 & \sigma_{\mathrm{H}} & 0 & -k_{12} & 0 & 0 \\ 0 & 0 & 0 & 0 & \sigma_{\mathrm{L}} & 0 & -k_{13} & 0 \\ \gamma_{\mathrm{A}} & \gamma_{\mathrm{TH}} & \gamma_{\mathrm{TL}} & \gamma_{\mathrm{HH}} & \gamma_{\mathrm{HL}} & \gamma_{\mathrm{CH}} & \gamma_{\mathrm{CL}} & -\mu \end{bmatrix},$$

where $\Upsilon_1 = \mu + \xi(1-\epsilon)$. It can be shown, from $J(\mathcal{E}_0)$, that (as before)

$$\mathcal{R}_c = \frac{\beta[S^* + (1-\epsilon)V^*](\Phi_1\tau_{\mathrm{H}} + \Phi_2\tau_{\mathrm{L}} + \Phi_3\kappa_{\mathrm{H}} + \Phi_4\kappa_{\mathrm{L}} + \Phi_5)}{N^* k_2k_3k_4k_5k_6k_7k_8k_9k_{10}k_{11}k_{12}k_{13}}.$$

Consider the case where $\mathcal{R}_c = 1$. Suppose, further, that β is chosen as a bifurcation parameter. Solving for β from $\mathcal{R}_c = 1$ gives

$$\beta = \beta_1^* = \frac{N^* k_2k_3k_4k_5k_6k_7k_8k_9k_{10}k_{11}k_{12}k_{13}}{[S^* + (1-\epsilon)V^*](\Phi_1\tau_{\mathrm{H}} + \Phi_2\tau_{\mathrm{L}} + \Phi_3\kappa_{\mathrm{H}} + \Phi_4\kappa_{\mathrm{L}} + \Phi_5)}. \tag{14}$$

It is easy to verify that the transformed system (12), with $\beta = \beta_1^*$, has a hyperbolic equilibrium point (i.e., the linearized system has a simple eigenvalue with zero real part, and all other eigenvalues have negative real parts). Hence, the centre manifold theory (Carr 1981) can be used to analyse the dynamics of (12) near $\beta = \beta_1^*$.

Eigenvectors of $J(\mathcal{E}_0)|_{\beta=\beta_1^*}$

It can be shown that the Jacobian of (12) at $\beta = \beta_1^*$ (denoted by $J_{\beta_1^*}$) has a right eigenvector (associated with the zero eigenvalue) given by $\mathbf{w} = [w_1, w_2, w_3, w_4, w_5, w_6, w_7, w_8, w_9, w_{10}, w_{11}, w_{12}, w_{13}, w_{14}, w_{15}]^{\mathrm{T}}$, where

$$w_1 = -\frac{\beta_1^*\mu\Upsilon_2}{k_1^2}, \qquad w_2 = \frac{\xi w_1}{\mu} - \frac{\beta_1^*\xi(1-\epsilon)\Upsilon_2}{\mu k_1}, \qquad w_3 = w_3 > 0,$$

$$w_4 = \frac{fr\alpha w_3}{k_3}, \qquad w_5 = \frac{(1-f)r\alpha w_3}{k_4},$$

$$w_6 = \frac{\kappa_{\mathrm{H}} w_4}{k_5}, \qquad w_7 = \frac{\kappa_{\mathrm{L}} w_5}{k_6}, \qquad w_8 = \frac{(1-r)\alpha w_3}{k_7},$$

$$w_9 = \frac{\tau_{\mathrm{H}} w_4}{k_8}, \qquad w_{10} = \frac{\tau_{\mathrm{L}} w_5}{k_9},$$

$$w_{11} = \frac{\psi_{\mathrm{H}} w_6 + \phi_{\mathrm{H}} w_9}{k_{10}}, \qquad w_{12} = \frac{\psi_{\mathrm{L}} w_7 + \phi_{\mathrm{L}} w_{10}}{k_{11}},$$

$$w_{13} = \frac{\sigma_{\mathrm{H}} w_{11}}{k_{12}}, \qquad w_{14} = \frac{\sigma_{\mathrm{L}} w_{12}}{k_{13}},$$

$$w_{15} = \frac{\gamma_{\mathrm{H}} w_6 + \gamma_{\mathrm{L}} w_7 + \gamma_{\mathrm{A}} w_8 + \gamma_{\mathrm{TH}} w_9 + \gamma_{\mathrm{TL}} w_{10} + \gamma_{\mathrm{HH}} w_{11}}{\mu} + \frac{\gamma_{\mathrm{HL}} w_{12} + \gamma_{\mathrm{CH}} w_{13} + \gamma_{\mathrm{CL}} w_{14}}{\mu},$$

with

$$\Upsilon_2 = w_3\theta_1 + w_4 + w_5\theta_2 + w_6\theta_3 + w_7\theta_4 + w_8\theta_5 + w_9\theta_6 + w_{10}\theta_7 + w_{11}\theta_8 + w_{12}\theta_9 + w_{13}\theta_{10} + w_{14}\theta_{11}.$$

Furthermore, $J_{\beta_1^*}$ has a left eigenvector $\mathbf{v} = [v_1, v_2, v_3, v_4, v_5, v_6, v_7, v_8, v_9, v_{10}, v_{11}, v_{12}, v_{13}, v_{14}, v_{15}]$ (associated with the zero eigenvalue), where

$$v_1 = 0, \qquad v_2 = 0, \qquad v_3 = v_3 > 0, \qquad v_4 = \frac{\beta_1^* \Upsilon_1 v_3}{k_1 k_3} + \frac{\kappa_{\mathrm{H}} v_6}{k_3} + \frac{\tau_{\mathrm{H}} v_9}{k_3},$$

$$v_5 = \frac{\beta_1^* \theta_2 \Upsilon_1 v_3}{k_1 k_4} + \frac{\kappa_{\mathrm{L}} v_7}{k_4} + \frac{\tau_{\mathrm{L}} v_{10}}{k_4}, \qquad v_6 = \frac{\beta_1^* \theta_3 \Upsilon_1 v_3}{k_1 k_5} + \frac{\psi_{\mathrm{H}} v_{11}}{k_5},$$

$$v_7 = \frac{\beta_1^* \theta_4 \Upsilon_1 v_3}{k_1 k_6} + \frac{\psi_{\mathrm{L}} v_{12}}{k_6}, \qquad v_8 = \frac{\beta_1^* \theta_5 \Upsilon_1 v_3}{k_1 k_7}, \qquad v_9 = \frac{\beta_1^* \theta_6 \Upsilon_1 v_3}{k_1 k_8} + \frac{\phi_{\mathrm{H}} v_{11}}{k_8},$$

$$v_{10} = \frac{\beta_1^* \theta_7 \Upsilon_1 v_3}{k_1 k_9} + \frac{\phi_{\mathrm{L}} v_{12}}{k_9}, \qquad v_{11} = \frac{\beta_1^* \theta_8 \Upsilon_1 v_3}{k_1 k_{10}} + \frac{\sigma_{\mathrm{H}} v_{13}}{k_{10}},$$

$$v_{12} = \frac{\beta_1^* \theta_9 \Upsilon_1 v_3}{k_1 k_{11}} + \frac{\sigma_{\mathrm{L}} v_{14}}{k_{11}},$$

$$v_{13} = \frac{\beta_1^* \theta_{10} \Upsilon_1 v_3}{k_{12}}, \qquad v_{14} = \frac{\beta_1^* \theta_{11} \Upsilon_1 v_3}{k_{13}}, \qquad v_{15} = 0.$$

The theorem in Castillo-Chavez and Song (2004) (see also Carr 1981; Dushoff et al. 1998; van den Driessche and Watmough 2002) is reproduced below for convenience.

Theorem A.1 (Castillo-Chavez and Song 2004) *Consider the following general system of ordinary differential equations with a parameter ϕ :*

$$\frac{dx}{dt} = f(x, \phi), \quad f: \quad \mathbb{R}^n \times \mathbb{R} \to \mathbb{R} \quad \textit{and} \quad f \in \mathbb{C}^2\big(\mathbb{R}^n \times \mathbb{R}\big), \tag{15}$$

where 0 *is an equilibrium point of the system* (*that is*, $f(0, \phi) \equiv 0$ *for all* ϕ), *and assume*

A1: $A = D_x f(0, 0) = (\frac{\partial f_i}{\partial x_j}(0, 0))$ *is the linearization matrix of system* (15) *around the equilibrium* 0 *with* ϕ *evaluated at* 0. *Zero is a simple eigenvalue of* A, *and other eigenvalues of* A *have negative real parts*;

A2: *Matrix* A *has a right eigenvector* w *and a left eigenvector* v (*each corresponding to the zero eigenvalue*).

Let f_k *be the* k*th component of* f, *and*

$$a = \sum_{k,i,j=1}^{n} v_k w_i w_j \frac{\partial^2 f_k}{\partial x_i \partial x_j}(0, 0),$$

$$b = \sum_{k,i=1}^{n} v_k w_i \frac{\partial^2 f_k}{\partial x_i \partial \phi}(0, 0).$$

The local dynamics of the system around 0 *is totally determined by the signs of* a *and* b.

(i) $a > 0, b > 0$. *When* $\phi < 0$ *with* $|\phi| \ll 1$, 0 *is locally asymptotically stable, and there exists a positive unstable equilibrium; when* $0 < \phi \ll 1$, 0 *is unstable, and there exists a negative, locally asymptotically stable equilibrium.*

(ii) $a < 0, b < 0$. *When* $\phi < 0$ *with* $|\phi| \ll 1$, 0 *is unstable; when* $0 < \phi \ll 1$, 0 *is locally asymptotically stable equilibrium, and there exists a positive unstable equilibrium.*

(iii) $a > 0, b < 0$. *When* $\phi < 0$ *with* $|\phi| \ll 1$, 0 *is unstable, and there exists a locally asymptotically stable negative equilibrium; when* $0 < \phi \ll 1$, 0 *is stable, and a positive unstable equilibrium appears.*

(iv) $a < 0, b > 0$. *When* ϕ *changes from negative to positive,* 0 *changes its stability from stable to unstable. Correspondingly, a negative unstable equilibrium becomes positive and locally asymptotically stable.*

Particularly, if $a > 0$ *and* $b > 0$, *then a backward bifurcation occurs at* $\phi = 0$.

Computations of a and b It can be shown, by computing the nonzero partial derivatives of F at the DFE $(\mathcal{E}_0)$ and simplifying, that

$$a = \sum_{k,i,j=1}^{n} v_k w_i w_j \frac{\partial^2 f_k}{\partial x_i \partial x_j}(0,0) = \frac{2\beta_1^* \mu v_3 \Upsilon_2}{k_1}\left[\frac{\epsilon \beta_1^* \xi (1-\epsilon)\Upsilon_2}{k_1} - \Upsilon_1 \sum_{i=1}^{11} w_i\right],$$

so that the bifurcation coefficient $a > 0$ if and only if

$$\beta_1^* > \frac{k_1 \Upsilon_1}{\epsilon \xi (1-\epsilon)\Upsilon_2} \sum_{i=1}^{11} w_i. \tag{16}$$

Furthermore, it can be shown that

$$b = \frac{v_3 \Upsilon_1 \Upsilon_2}{k_1} > 0.$$

Thus, it follows from Theorem 5 that:

Theorem A.2 *Model* (12) (*or, equivalently, model* (2)) *undergoes a backward bifurcation at* $\mathcal{R}_c = 1$ *if inequality* (16) *holds.*

□

It is worth noting from the equation for a above that if the vaccine is perfect (i.e., $\epsilon = 1$), the bifurcation coefficient $a < 0$. Thus, backward bifurcation phenomenon is not feasible in this case (this is in line with Theorem 4).

References

Boëlle, P. Y., Bernillon, P., & Desenclos, J. C. (2000). A preliminary estimation of the reproduction ratio for new influenza A(H1N1) from the outbreak in Mexico. *Euro Surveill.*, *14*(19), 19205.

Brauer, F. (2004). Backward bifurcations in simple vaccination models. *J. Math. Anal. Appl.*, *298*(2), 418.

Brian, J. C., Bradley, G. W., & Sally, B. (2009). Modeling influenza epidemics and pandemics: insights into the future of swine flu (H1N1). *BMC Med.* doi:10.1186/1741-7015-7-30.

Canada Enters Second Wave of H1N1. http://www.cbc.ca/health/story/2009/10/23/h1n1-second-wave-canada.html. Accessed 04 November 2009.

Carr, J. (1981). *Applications Centre Manifold Theory*. New York: Springer.

Castillo-Chavez, C., & Song, B. (2004). Dynamical models of tuberculosis and their applications. *Math. Biosci. Eng.*, *1*(2), 361–404.

Castillo-Chavez, C., Cooke, K., Huang, W., & Levin, S. A. (1989a). Results on the dynamics for models for the sexual transmission of the human immunodeficiency virus. *Appl. Math. Lett.*, *2*, 327.

Castillo-Chavez, C., Cooke, K., Huang, W., & Levin, S. A. (1989b). The role of long incubation periods in the dynamics of HIV/AIDS. Part 2: Multiple group models). In C. Castillo-Chavez (Ed.), *Lecture notes in biomathematics: Vol. 83. Mathematical and statistical approaches to AIDS epidemiology* (p. 200). Berlin: Springer.

Centers for Disease Control and Prevention (2009a). http://www.cdc.gov/h1n1flu/background.htm. Accessed 27 October 2009.

Centers for Disease Control and Prevention (2009b). http://www.cdc.gov/h1n1flu/recommendations.htm. Accessed 27 October 2009.

Centers for Disease Control and Prevention (2009c). http://www.cdc.gov/media/pressrel/2009/r090729b.htm. Accessed 27 October 2009.

Centers for Disease Control and Prevention (2009d). Outbreak of swine-origin influenza A (H1N1) virus infection-Mexico, March–April 2009. *Morb. Mort. Wkly. Rep.*, *58*, 1–3.

Centers for Disease Control and Prevention (2009e). http://www.cdc.gov/h1n1flu/identifyingpatients.htm#incubationperiod. Accessed 27 October 2009.

Chowell, G., et al. (2009). Severe respiratory disease concurrent with the circulation of H1N1 influenza. *N. Engl. J. Med.*, *361*, 674–679.

Cox, N., Bridges, C., Levandowski, R., & Katz, J. (2008). Influenza vaccine (inactivated). In S. Plotkin, W. Orenstein, & P. Offit (Eds.), *Vaccines* (pp. 259–290). Amsterdam: Elsevier.

Demicheli, V., Di Pietrantonj, C., Jefferson, T., Rivetti, A., & Rivetti, D. (2009). *Vaccines for preventing influenza in healthy adults (review). The Cochrane collaboration*. New York: Wiley.

Dushoff, J., Wenzhang, H., & Castillo-Chavez, C. (1998). Backwards bifurcations and catastrophe in simple models of fatal diseases. *J. Math. Biol.*, *36*, 227–248.

El Universal, 6 April 2009. http://www.eluniversal.com.mx/hemeroteca/edicion_impresa_20090406.html. Accessed 27 October 2009.

Elbasha, E. H., & Gumel, A. B. (2006). Theoretical assessment of public health impact of imperfect prophylactic HIV-1 vaccines with therapeutic benefits. *Bull. Math. Biol.*, *68*, 577–614.

Feng, Z., Castillo-Chavez, C., & Capurro, F. (2000). A model for tuberculosis with exogenous reinfection. *Theor. Popul. Biol.*, *57*, 235.

FluWatch (2010). Weekly reports 2009–2010 season. http://www.phac-aspc.gc.ca/fluwatch/index-eng.php. Accessed 11 January 2010.

Franco-Paredes, P. C., & Preciado, J. I. S. (2009). The first influenza pandemic in the new millennium: lessons learned hitherto for current control efforts and overall pandemic preparedness. *J. Immune Based Therap. Vaccines*. doi:10.1186/1476-8518-7-2.

Fraser, C., Donnelly, C. A., Cauchemez, S., et al. (2009). Pandemic potential of a strain of influenza A (H1N1): early findings. *Science*, *324*, 1557–1561.

GenBank (2009). Sequences from 2009 H1N1 influenza outbreak. http://www.ncbi.nlm.nih.gov/genomes/FLU/SwineFlu.html. Accessed 27 October 2009.

Gomez-Acevedo, H., & Li, M. Y. (2005). Backward bifurcation in a model for HTLV-I infection of CD4+ T cells. *Bull. Math. Biol.*, *67*(1), 101.

Greenberg, M. E., Lai, M. H., Hartel, G. F., Wichems, C. H., Gittleson, C., Bennet, J., Dawson, G., Hu, W., Leggio, C., Washington, D., & Basser, R. L. (2009). Response after one dose of a monovalent influenza A (H1N1) 2009 vaccine—preliminary report. *N. Engl. J. Med.*, *361*(25), 2405–2413.

Gumel, A. B., Nuno, M., & Chowell, G. (2008). Mathematical assessment of Canada's pandemic preparedness plan. *Can. J. Infect. Dis. Med. Microbiol.*, *19*(2), 185–192.

Hadeler, K. P., & Castillo-Chavez, C. (1995). A core group model for disease transmission. *Math. Biosci.*, *128*, 41.

Hale, J. K. (1969). *Ordinary differential equations*. New York: Wiley.

Hethcote, H. W. (2000). The mathematics of infectious diseases. *SIAM Rev.*, *42*(4), 599–653.

Hiroshi, N., Don, K., Mick, R., & Johan, A. P. H. (2009). Early epidemiological assessment of the virulence of emerging infectious diseases: a case study of an influenza pandemic. *PLoS ONE*. doi:10.1371/journal.pone.0006852.s001.

Jamieson, D. J., Honein, M. A., Rasmussen, S. A., et al. (2009). H1N1 2009 influenza virus infection during pregnancy in the USA. *Lancet*, *374*(9688), 451–458.

Kribs-Zaleta, C., & Valesco-Hernandez, J. (2000). A simple vaccination model with multiple endemic states. *Math. Biosci.*, *164*, 183.

Kumar, A., Zarychanski, R., Pinto, R., et al. (2009). Critically ill patients with 2009 influenza A(H1N1) infection in Canada. *JAMA*, *302*(17), 1872–1879. doi:10.1001/jama.2009.1496

Lakshmikantham, V., Leela, S., & Martynyuk, A. A. (1989). *Stability analysis of nonlinear systems*. New York: Marcel Dekker.

Lipsitch, M., & Murray, M. B. (2003). Multiple equilibria: tuberculosis transmission require unrealistic assumptions. *Theor. Popul. Biol.*, *63*(2), 169–170.

Mahmud, S. M., Becker, M., Keynan, Y., Elliot, L., et al. (2010, submitted). Serological survey of the pandemic influenza A H1N1 in Manitoba, Summer 2009. *J. Infect. Dis.*

Manitoba Health (2009). Confirmed cases of H1N1 flu in Manitoba. http://www.gov.mb.ca/health/publichealth/sri/cases.html. Accessed 27 October 2009.

Miriam, N., Chowell, G., & Gumel, A. B. (2007). Assessing transmission control measures, antivirals and vaccine in curtailing pandemic influenza: scenarios for the US, UK, and the Netherlands. *Proc. R. Soc. Interface*, *4*(14), 505–521.

Nishiura, H., Castillo-Chavez, C., Safan, M., & Chowell, G. (2009). Transmission potential of the new influenza A(H1N1) virus and its age-specificity in Japan. *Euro Surveill.*, *14*, 19227.

Podder, C. N., & Gumel, A. B. (2009). Qualitative dynamics of a vaccination model for HSV-2. *IMA J. Appl. Math.* doi:10.1093/imamat/hxp030.

Pourbohloul, B., et al. (2009). Initial human transmission dynamics of the pandemic (H1N1) 2009 virus in North America. *Influenza Other Respir. Viruses*, *3*(5), 215–222.

Sharomi, O., & Gumel, A. B. (2009). Re-infection-induced backward bifurcation in the transmission dynamics of Chlamydia trachomatis. *J. Math. Anal. Appl.*, *356*, 96–118.

Sharomi, O., Podder, C. N., Gumel, A. B., Elbasha, E. H., & Watmough, J. (2007). Role of incidence function in vaccine-induced backward bifurcation in some HIV models. *Math. Biosci.*, *210*, 436–463.

Sharomi, O., Podder, C. N., Gumel, A. B., & Song, B. (2008). Mathematical analysis of the transmission dynamics of HIV/TB co-infection in the presence of treatment. *Math. Biosci. Eng.*, *5*(1), 145–174.

Simon, C. P., & Jacquez, J. A. (1992). Reproduction numbers and the stability of equilibrium of SI models for heterogeneous populations. *SIAM J. Appl. Math.*, *52*, 541.

Statistics Canada (2009a). Population urban and rural, by province and territory (Manitoba). http://www40.statcan.gc.ca/l01/cst01/demo62h-eng.htm. Accessed 27 October 2009.

Statistics Canada (2009b). Life expectancy at birth, by sex, by province. http://www40.statcan.gc.ca/l01/cst01/health26-eng.htm. Accessed 27 October 2009.

United States Centers for Disease Control and Prevention (2009). Pregnant women and novel influenza A (H1N1): considerations for clinicians. http://www.cdc.gov/h1n1flu/clinician_pregnant.htm. Accessed 5 November 2009.

United States Centers for Disease Control (2009). Information on people at high risk of developing flu-related complications. http://www.cdc.gov/h1n1flu/highrisk.htm. Accessed 5 November 2009.

van den Driessche, P., & Watmough, J. (2002). Reproduction numbers and sub-threshold endemic equilibria for compartmental models of disease transmission. *Math. Biosci.*, *180*, 29–48.

van der Vries, E., Jonges, M., Herfst, S., Maaskant, J., Van der Linden, A., Guldemeester, J., Aron, G.I., Bestebroer, T.M., Koopmans, M., Meijer, A., Fouchier, R.A., Osterhaus, A.D., Boucher, C.A., & Schutten, M. (2009). Evaluation of a rapid molecular algorithm for detection of pandemic influenza A (H1N1) 2009 virus and screening for a key oseltamivir resistance (H275Y) substitution in neuraminidase. *Clin. Virol.* doi:10.1016/j.jcv.2009.09.030.

Wang, W. (2006). Backward bifurcation of an epidemic model with treatment. *Math. Biosci.*, *201*(1–2), 58.

Winnipeg Regional Health Authority Report (2009). Outbreak of novel H1N1 influenza A virus in the Winnipeg health region. http://www.wrha.mb.ca/. Accessed 4 November 2009.

World Health Organization (2009a). Pandemic (H1N1) (2009)—update 71. http://www.who.int/csr/don/2009_10_23/en/index.html. Accessed 27 October 2009.

World Health Organization (2009b). Influenza A (H1N1)—update 49. Global Alert and Response (GAR). http://www.who.int/csr/don/2009_06_15/en/index.html. Accessed 27 October 2009.

World Health Organization (2009c). Statement by Director-General. 11 June 2009.
World Health Organization (2009d). Pandemic (H1N1) (2009)—update 72. http://www.who.int/csr/don/2009_10_30/en/index.html. Accessed 31 October 2009.
World Health Organization (2009e). Human infection with pandemic A (H1N1) 2009 infuenza virus: clinical observations in hospitalized patients, Americas, July 2009—update. *Wkly. Epidemiol. Rec. 84*, 305–308.
World Health Organization (2009f). Alert and response: http://www.who.int/csr/disease/swineflu/updates/en/index.html. Accessed 02 November 2009.
World Health Organization (2009g). Human infection with new influenza A (H1N1) virus: clinical observations from Mexico and other affected countries. *Wkly. Epidemiol. Rec.*, *84*, 185. http://www.who.int/wer/2009/wer8421.pdf. Accessed 5 November 2009.